Contents lists available at ScienceDirect

Physics Letters B

www.elsevier.com/locate/physletb

Search for lepton flavour violating decays of the Higgs boson to eτ and eμ in proton–proton collisions at $\sqrt{s} = 8$ TeV

The CMS Collaboration[*]

CERN, Switzerland

A B S T R A C T

A direct search for lepton flavour violating decays of the Higgs boson (H) in the $H \to e\tau$ and $H \to e\mu$ channels is described. The data sample used in the search was collected in proton–proton collisions at $\sqrt{s} = 8$ TeV with the CMS detector at the LHC and corresponds to an integrated luminosity of 19.7 fb^{-1}. No evidence is found for lepton flavour violating decays in either final state. Upper limits on the branching fractions, $\mathcal{B}(H \to e\tau) < 0.69\%$ and $\mathcal{B}(H \to e\mu) < 0.035\%$, are set at the 95% confidence level. The constraint set on $\mathcal{B}(H \to e\tau)$ is an order of magnitude more stringent than the existing indirect limits. The limits are used to constrain the corresponding flavour violating Yukawa couplings, absent in the standard model.

© 2016 The Author(s). Published by Elsevier B.V. This is an open access article under the CC BY license (http://creativecommons.org/licenses/by/4.0/). Funded by SCOAP^3.

1. Introduction

The discovery of the Higgs boson [1–3] has generated great interest in exploring its properties. In the standard model (SM), lepton flavour violating (LFV) decays of the Higgs boson are forbidden. Such decays can occur naturally in models with more than one Higgs boson doublet [4]. They also arise in supersymmetric models [5–11], composite Higgs models [12,13], models with flavour symmetries [14], Randall–Sundrum models [15–17], and others [18–26]. The CMS Collaboration has recently published a search in the $H \to \mu\tau$ channel [27] showing an excess of data with respect to the SM background-only hypothesis at $m_H = 125$ GeV with a significance of 2.4 standard deviations (σ). A constraint is set on the branching fraction $\mathcal{B}(H \to \mu\tau) < 1.51\%$ at 95% confidence level (CL), while the best fit branching fraction is $\mathcal{B}(H \to \mu\tau) = (0.84^{+0.39}_{-0.37})\%$. The ATLAS Collaboration finds a deviation from the background expectation of 1.3σ significance in the $H \to \mu\tau$ channel and sets an upper limit of $\mathcal{B}(H \to \mu\tau) < 1.85\%$ at 95% CL with a best fit branching fraction of $\mathcal{B}(H \to \mu\tau) = (0.77 \pm 0.62)\%$ [28]. To date, no dedicated searches have been published for the $H \to e\mu$ channel. The ATLAS Collaboration recently reported searches for $H \to e\tau$ and $H \to \mu\tau$, finding no significant excess of events over the background expectation. The searches in channels with leptonic tau decays are sensitive only to a difference between $\mathcal{B}(H \to e\tau)$ and $\mathcal{B}(H \to \mu\tau)$. These are

combined with the searches in channels with hadronic tau decays to set limits of $\mathcal{B}(H \to e\tau) < 1.04\%$, $\mathcal{B}(H \to \mu\tau) < 1.43\%$ at 95% CL [29]. There are also indirect constraints. The presence of LFV Higgs boson couplings allows, $\mu \to e$, $\tau \to \mu$, and $\tau \to e$ to proceed via a virtual Higgs boson [30,31]. The experimental limits on these decays have been translated into constraints on $\mathcal{B}(H \to e\mu)$, $\mathcal{B}(H \to \mu\tau)$ and $\mathcal{B}(H \to e\tau)$ [32,33]. The null result for $\mu \to e\gamma$ [34] strongly constrains $\mathcal{B}(H \to e\mu) < \mathcal{O}(10^{-8})$. However, the constraint $\mathcal{B}(H \to e\tau) < \mathcal{O}(10\%)$ is much less stringent. This comes from searches for rare τ decays [35] such as $\tau \to e\gamma$, and the measurement of the electron magnetic moment. Exclusion limits on the electric dipole moment of the electron [36] also provide complementary constraints.

This letter describes a search for LFV decays of the Higgs boson with $m_H = 125$ GeV, based on proton–proton collision data recorded at $\sqrt{s} = 8$ TeV with the CMS detector at the CERN LHC, corresponding to an integrated luminosity of 19.7 fb^{-1}. The search is performed in three decay channels, $H \to e\tau_\mu$, $H \to e\tau_h$, and $H \to e\mu$, where τ_μ and τ_h correspond to muonic and hadronic decay channels of tau leptons, respectively. The decay channel, $H \to e\tau_e$, is not considered due to the large background contribution from $Z \to ee$ decays. The expected final state signatures are very similar to the SM $H \to \tau_e\tau_h$ and $H \to \tau_e\tau_\mu$ decays, studied by CMS [37,38] and ATLAS [39], but with some significant kinematic differences. The electron in the LFV $H \to e\tau$ decay is produced promptly, and tends to have a larger momentum than in the SM $H \to \tau_e\tau_h$ decay. In the $H \to e\mu$ channel, m_H can be measured with good resolution due to the absence of neutrinos.

This letter is organized as follows. After a description of the CMS detector (Section 2) and of the collision data and simulated samples used in the analysis (Section 3), the event reconstruction is described in Section 4. The event selection and the estimation of the background and its components are described separately for the two Higgs decay modes H → eτ and H → eμ in Sections 5 and 6. The results are then presented in Section 7.

2. The CMS detector

A detailed description of the CMS detector, together with a definition of the coordinate system used and the relevant kinematic variables, can be found in Ref. [40]. The momenta of charged particles are measured with a silicon pixel and strip tracker that covers the pseudorapidity range $|\eta| < 2.5$, in a 3.8 T axial magnetic field. A lead tungstate crystal electromagnetic calorimeter (ECAL) and a brass and scintillator hadron calorimeter, both consisting of a barrel section and two endcaps, cover the pseudorapidity range $|\eta| < 3.0$. A steel and quartz-fibre Cherenkov forward detector extends the calorimetric coverage to $|\eta| < 5.0$. The outermost component of the CMS detector is the muon system, consisting of gas-ionization detectors placed in the steel flux-return yoke of the magnet to identify the muons traversing the detector. The two-level CMS trigger system selects events of interest for permanent storage. The first trigger level, composed of custom hardware processors, uses information from the calorimeters and muon detectors to select events in less than 3.2 μs. The software algorithms of the high-level trigger, executed on a farm of commercial processors, reduce the event rate to less than 1 kHz using information from all detector subsystems.

3. Collision data and simulated events

The triggers for the H → eτ$_\mu$ and H → eμ analyses require an electron and a muon candidate. The trigger for H → eτ$_h$ requires a single electron. More details on the trigger selection are given in Sections 5.1 and 6.1, for the H → eτ and H → eμ channels respectively. Simulated samples of signal and background events are produced with several event generators. The CMS detector response is modelled using GEANT4 [41]. The Higgs bosons are produced in proton–proton collisions predominantly by gluon fusion (GF) [42], but also by vector boson fusion (VBF) [43] and in association with a W or Z boson [44]. The H → eτ decay sample is produced with PYTHIA 8.176 [45] using the CTEQ6L parton distribution functions (PDF). The H → eμ decay sample is produced with PYTHIA 6.426 [46] using the CT10 parton distribution functions [47]. The SM Higgs boson samples are generated using POWHEG 1.0 [48–52], with CT10 parton distribution functions, interfaced to PYTHIA 6.426. The MADGRAPH 5.1.3.30 [53] generator is used for Z+jets, W+jets, top anti-top quark pair production t$\bar{\text{t}}$, and diboson production, and POWHEG for single top quark production. The POWHEG and MAD-GRAPH generators are interfaced to PYTHIA 6.426 for parton shower and hadronization. The PYTHIA parameters for the underlying event description are set to the Z2* tune. The Z2* tune is derived from the Z1 tune [54], which uses the CTEQ5L parton distribution set, whereas Z2* adopts CTEQ6L. Due to the high luminosities attained during data-taking, many events have multiple proton–proton interactions per bunch crossing (pileup). All simulated samples are reweighted to match the pileup distribution observed in data.

4. Event reconstruction

Data were collected at an average pileup of 21 interactions per bunch crossing. The tracking system is able to separate collision vertices as close as 0.5 mm to each other along the beam direction [55]. The primary vertex, assumed to correspond to the hard-scattering process, is the vertex for which the sum of the squared transverse momentum p_T^2 of all the associated tracks is the largest. The pileup interactions also affect the identification of most of the physics objects, such as jets, and variables such as lepton isolation.

A particle-flow (PF) algorithm [56–58] combines the information from all CMS subdetectors to identify and reconstruct the individual particles emerging from all interactions in the event: charged and neutral hadrons, photons, muons, and electrons. These particles are then required to be consistent with the primary vertex and used to reconstruct jets, hadronic τ decays, quantify the isolation of leptons and photons and reconstruct $\vec{E}_T^{\text{miss}}$. The missing transverse energy vector, $\vec{E}_T^{\text{miss}}$, is defined as the negative of the vector sum of the p_T of all identified PF objects in the event [59]. Its magnitude is referred to as E_T^{miss}. The variable $\Delta R = \sqrt{(\Delta \eta)^2 + (\Delta \phi)^2}$, where ϕ is the azimuthal co-ordinate, is used to measure the separation between reconstructed objects in the detector.

Electron reconstruction requires the matching of an energy cluster in the ECAL with a track in the silicon tracker [60]. Electron candidates are accepted in the range $|\eta| < 2.5$, with the exception of the region $1.44 < |\eta| < 1.56$ where service infrastructure for the detector is located. Electron identification uses a multivariate discriminant that combines observables sensitive to the amount of bremsstrahlung along the electron trajectory, the geometrical and momentum matching between the electron trajectory and associated clusters, and shower-shape observables. Additional requirements are imposed to remove electrons produced by photon conversions. The electron energy is corrected for imperfection of the reconstruction using a regression based on a boosted decision tree [61].

Muon candidates are obtained from combined fits of tracks in the tracker and muon detector seeded by track segments in the muon detector alone, including compatibility with small energy depositions in the calorimeters. Identification is based on track quality and isolation. The muon momentum is estimated with the combined fit. Any possible bias in the measured muon momentum is determined from the position of the Z → μμ mass peak as a function of muon kinematic variables, and a small correction is obtained using the procedure described in Ref. [62].

Hadronically decaying τ leptons are reconstructed and identified using an algorithm [63] that selects the decay modes with one charged hadron and up to two neutral pions, or three charged hadrons. A photon from a neutral–pion decay can convert in the tracker material into an electron–positron pair, which can then radiate photons. These particles give rise to several ECAL energy deposits at the same η value but separated in ϕ. They are reconstructed as several photons by the PF algorithm. To increase the acceptance for these converted photons, the neutral pions are identified by clustering the reconstructed photons in narrow strips along the ϕ direction. The charge of τ_h candidates is reconstructed by summing the charges of all particles included in the construction of the candidate, except for the electrons contained in strips. Dedicated discriminators veto against electrons and muons.

Jets misidentified as electrons, muons or taus are suppressed by imposing isolation requirements, summing the neutral and charged particle contributions in cones of ΔR about the lepton. The energy deposited within the isolation cone is contaminated by energy from pileup and the underlying event. The effect of pileup is reduced by requiring the tracks considered in the isolation sum to be compatible with originating from the production vertex of the lepton. The contribution to the isolation from pileup and the underlying event is subtracted on an event-by-event basis. In the case

of electrons, this contribution is estimated from the product of the measured energy density ρ for the event, determined using the ρ median estimator implemented in FASTJET [64], and an effective area corresponding to the isolation cone. In the case of muons and hadronically decaying τ leptons, it is estimated on a statistical basis through the modified $\Delta\beta$ correction described in Ref. [63].

Jets are reconstructed from all the particles using the anti-k_T jet clustering algorithm [65] implemented in FASTJET, with a distance parameter of $\Delta R = 0.5$. The jet energies are corrected by subtracting the contribution of particles created in pileup interactions and in the underlying event [66]. Particles from different pileup vertices can be clustered into a pileup jet, or significantly overlap a jet from the primary vertex below the selected jet p_T threshold. These jets are identified and removed [67].

5. H → eτ analysis

5.1. Event selection

The H → eτ_h selection begins by requiring an event recorded with a single electron trigger ($p_T^e > 27$ GeV, $|\eta^e| < 2.5$). The H → eτ_μ channel requires a muon–electron trigger ($p_T^e > 17$ GeV, $|\eta^e| < 2.5$, $p_T^\mu > 8$ GeV, $|\eta^\mu| < 2.4$). The triggers also apply loose identification and isolation requirements to the leptons.

A loose selection is then made for both channels. Electron, muon and hadronic tau lepton candidates are required to be isolated and to lie in the pseudorapidity ranges where they can be well reconstructed; $|\eta^e| < 1.44$ or $1.57 < |\eta^e| < 2.30$, $|\eta^\mu| < 2.1$ and $|\eta^{\tau_h}| < 2.3$, respectively. Leptons are also required to be compatible with the primary vertex and to be separated by $\Delta R > 0.4$ from any jet in the event with $p_T > 30$ GeV. The H → eτ_μ channel then requires an electron ($p_T^e > 40$ GeV) and an oppositely charged muon ($p_T^\mu > 10$ GeV) separated by $\Delta R > 0.1$. Events in this channel with additional muons ($p_T > 7$ GeV) or electrons ($p_T > 7$ GeV) are also rejected. The H → eτ_h channel requires an electron ($p_T^e > 30$ GeV) and an oppositely charged hadronic tau lepton ($p_T^{\tau_h} > 30$ GeV). Events in this channel with additional muons ($p_T > 5$ GeV), electrons ($p_T > 10$ GeV), or hadronic tau leptons ($p_T > 20$ GeV) are rejected.

The events are then divided into categories within each channel according to the number of jets in the event. Jets are required to pass identification criteria, have $p_T > 30$ GeV, and lie in the region $|\eta| < 4.7$. The 0-jet and 1-jet categories contain events primarily produced by GF. The 2-jet category is defined to enrich the contribution from events produced via the VBF process.

The main observable used to discriminate between the signal and the background is the collinear mass, M_{col}, which provides an estimate of M_H using the observed decay products. It is constructed using the collinear approximation based on the observation that, since $m_H \gg M_\tau$, the τ decay products are highly Lorentz boosted in the direction of the τ [68]. The neutrino momenta can be approximated to have the same direction as the other visible decay products of the τ (τ^{vis}) and the component of the $\vec{E}_T^{miss}$ in the direction of the visible τ decay products is used to estimate the transverse component of the neutrino momentum ($p_T^{\nu,\ est}$). The collinear mass can then be derived from the visible mass of the τ–e system (M_{vis}) as $M_{col} = M_{vis}/\sqrt{x_\tau^{vis}}$, where x_τ^{vis} is the fraction of energy carried by the visible decay products of the τ ($x_\tau^{vis} = p_T^{\tau^{vis}}/(p_T^{\tau^{vis}} + p_T^{\nu,\ est})$).

Fig. 1 shows the observed M_{col} distribution and estimated backgrounds for each category and channel, after the loose selection. The simulated signal for $\mathcal{B}(H \to e\tau) = 100\%$ is shown. The principal backgrounds are estimated with collision data using techniques described in Section 5.2. There is good agreement between the observed distributions and the corresponding background estimations. The agreement is similar in all of the kinematic variables that are subsequently used to suppress backgrounds. The analysis is subsequently performed blinded by using a fixed selection and checking the agreement between relevant observed and simulated distributions outside the sensitive region 100 GeV < M_{col} < 150 GeV.

Next, a set of kinematic variables is defined, and the event selection criteria are set to maximise the significance S/$\sqrt{S + B}$, where S and B are the expected signal and background event yields in the mass window 100 GeV < M_{col} < 150 GeV. The signal event yield corresponds to the SM Higgs boson production cross section at $m_H = 125$ GeV with $\mathcal{B}(H \to e\tau) = 1\%$. The selection criteria for each category and channel are given in Table 1. The variables used are: the lepton transverse momenta p_T^ℓ with $\ell = $ e, μ, τ_h; azimuthal angles between the leptons $\Delta\phi_{\vec{p}_T^{\ell_1} - \vec{p}_T^{\ell_2}}$; azimuthal angle between the lepton and the E_T^{miss} vector $\Delta\phi_{\vec{p}_T^\ell - \vec{E}_T^{miss}}$; the transverse mass $M_T^\ell = \sqrt{2p_T^\ell E_T^{miss}(1 - \cos\Delta\phi_{\vec{p}_T^\ell - \vec{E}_T^{miss}})}$.

Events in which at least one of the jets is identified as arising from a b quark decay are vetoed using the combined secondary vertex (CSV) b-tagging algorithm [69]. To enhance the VBF contribution in the 2-jet category further requirements are applied. In the H → eτ_h channel, events in this category are additionally required to have two jets separated by $|\Delta\eta| > 2.3$ and a dijet invariant mass $M_{jj} > 400$ GeV. In the H → eτ_μ channel, the requirements are $|\Delta\eta| > 3$ and $M_{jj} > 200$ GeV.

After the full selection, a binned likelihood is used to fit the distributions of M_{col} for the signal and the background contributions. The modified-frequentist CL$_s$ method [70,71] is used to set upper bounds on the signal strength μ, or determine a signal significance.

5.2. Background processes

The contributions from the dominant background processes are estimated using collision data while the less significant backgrounds are estimated using simulation. The largest backgrounds are from Z → $\tau\tau$ decays and from W + jets and QCD multijet production. In the latter, PF objects (predominantly jets), are misidentified as leptons.

5.2.1. Z → $\tau\tau$ background

The Z → $\tau\tau$ background contribution is estimated using an embedding technique [38,72]. First, a sample of Z → $\mu\mu$ events is selected from collision data using the loose muon selection. The muons are then replaced with simulated τ decays reconstructed with the PF algorithm. Thus, the key features of the event topology such as jet multiplicity, instrumental sources of E_T^{miss}, and the underlying event are taken directly from collision data. Only the τ lepton decays are simulated. The normalization of the sample is obtained from simulation. The technique is validated by comparing the collinear mass distributions obtained from the Z → $\tau\tau$ simulation and the embedding technique applied to a simulated sample of Z → $\mu\mu$ events. A shift of 2% in the mass peak of the embedded sample relative to simulation is observed. This shift reflects a bias in the embedding technique, which does not take the differences between muons and taus in final-state radiation of photons into account, and is corrected for. Identification and isolation corrections obtained from the comparison are applied to the embedded sample.

5.2.2. Misidentified lepton background

The misidentified lepton background is estimated from collision data by defining a sample with the same selection as the sig-
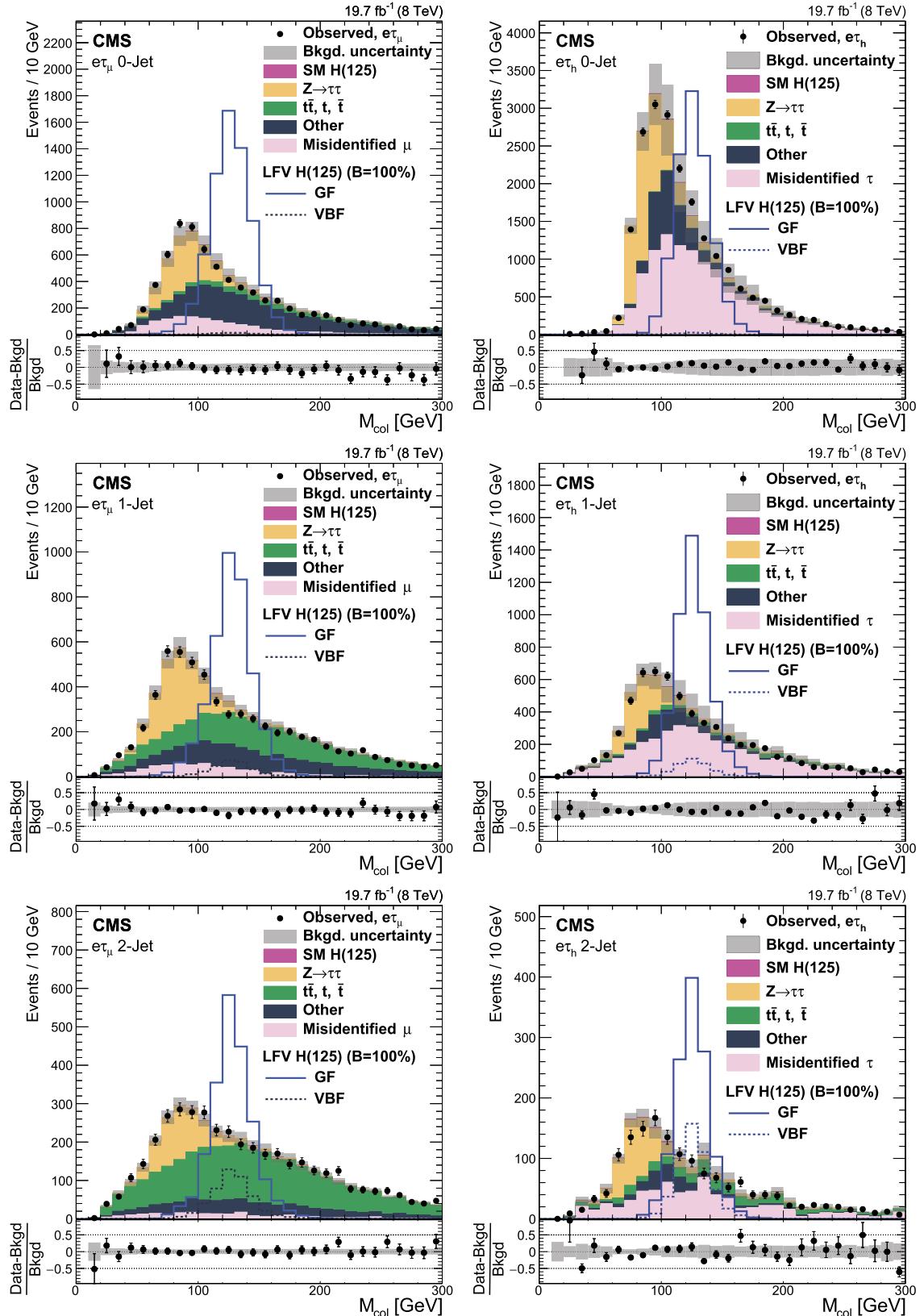
Fig. 1. Comparison of the observed collinear mass distributions with the background expectations after the loose selection requirements. The shaded grey bands indicate the total background uncertainty. The open histograms correspond to the expected signal distributions for $\mathcal{B}(H \rightarrow e\tau) = 100\%$. The left column is $H \rightarrow e\tau_\mu$ and the right column is $H \rightarrow e\tau_h$; the upper, middle and lower rows are the 0-jet, 1-jet and 2-jet categories, respectively.

Table 1
Event selection criteria for the kinematic variables after applying loose selection requirements.

Variable [GeV]	$H \to e\tau_\mu$			$H \to e\tau_h$		
	0-jet	1-jet	2-jet	0-jet	1-jet	2-jet
p_T^e	>50	>40	>40	>45	>35	>35
p_T^μ	>15	>15	>15	–	–	–
$p_T^{\tau_h}$	–	–	–	>30	>40	>30
M_T^μ	–	<30	<40	–	–	–
$M_T^{\tau_h}$	–	–	–	<70	–	<50
[radians]						
$\Delta\phi_{\vec{p}_{T,e}-\vec{p}_{T,\tau_h}}$	–	–	–	>2.3	–	–
$\Delta\phi_{\vec{p}_{T,\mu}-\vec{E}_T^{miss}}$	<0.8	<0.8	–	–	–	–
$\Delta\phi_{\vec{p}_{T,e}-\vec{p}_{T,\mu}}$	–	>0.5	–	–	–	–

Table 2
Definition of the samples used to estimate the misidentified lepton (ℓ) background. They are defined by the charge of the two leptons and by the isolation requirements on each. The definition of not-isolated differs between the two channels.

Region I	Region II
$\ell_1^\pm$ (isolated)	$\ell_1^\pm$ (isolated)
$\ell_2^\mp$ (isolated)	$\ell_2^\pm$ (isolated)

Region III	Region IV
$\ell_1^\pm$ (isolated)	$\ell_1^\pm$ (isolated)
$\ell_2^\mp$ (not-isolated)	$\ell_2^\pm$ (not-isolated)

nal sample, but inverting the isolation requirements on one of the leptons, to enrich the contribution from W + jets and QCD multi-jets. The probability for PF objects to be misidentified as leptons is measured using an independent collision data set, defined below, and this probability is applied to the background enriched sample to compute the misidentified lepton background in the signal sample. The technique is shown schematically in Table 2 in which four regions are defined including the signal (I) and background (III) enriched regions and two control Regions (II & IV), defined with the same selections as Regions I & III respectively, except with leptons of the same charge.

The misidentified electron background is negligible in the $H \to e\tau_\mu$ channel due to the high p_T electron threshold. The misidentified muon background is estimated with Region I defined as the signal selection with an isolated electron and an isolated muon of opposite charge. Region III is defined as the signal selection except the muon is required not to be isolated. Small background sources of prompt leptons are subtracted using simulation. The misidentified muon background in Region I is then estimated by multiplying the event yield in Region III by a factor f_μ, where f_μ is the ratio of isolated to nonisolated muons. It is computed on an independent collision data sample of $Z \to \mu\mu + X$ events, where X is an object identified as a muon, in bins of muon p_T and η. In the estimation of f_μ, background sources of three prompt leptons, predominantly WZ and ZZ, are subtracted from the $Z \to \mu\mu + X$ sample using simulation. The technique is validated using like-sign lepton collision data in Regions II and IV. In Fig. 2 (left) the event yield in Region II is compared to the estimate from scaling the Region IV sample by the measured misidentification rate. The Region II sample is dominated by misidentified leptons but also includes small contributions of true leptons arising from vector boson decays, estimated with simulated samples.

In the $H \to e\tau_h$ channel either lepton candidate can arise from a misidentified PF object, predominantly in W + jets and QCD multijet events, but also from $Z \to ee + jets$ and $t\bar{t}$ production. The misidentification rates f_τ and f_e are defined as the fraction of loosely isolated τ_h or electron candidates that also pass a tight isolation requirement. This is measured in $Z \to ee + X$ collision data events, where X is an object identified as a τ_h or e. The misidentified τ_h contribution is estimated with Region I defined as the signal selection. Region III is the signal selection except the τ_h is required to have loose and not tight isolation. The misidentified τ_h lepton background in Region I is then estimated by multiplying the event yield in Region III by a factor $f_\tau/(1-f_\tau)$. The same procedure is used to estimate the misidentified electron background by defining Region I as the signal selection and Region III as the signal selection but with a loose and not tight isolated electron, and scaling by $f_e/(1-f_e)$. To avoid double counting, the event yield in Region III, multiplied by a factor $f_e/(1-f_e) \times f_\tau/(1-f_\tau)$, is subtracted from the sum of misidentified electrons and taus. The procedure is validated with the like-sign $e\tau$ samples. Fig. 2 (right) shows the collision data in Region II compared to the estimate
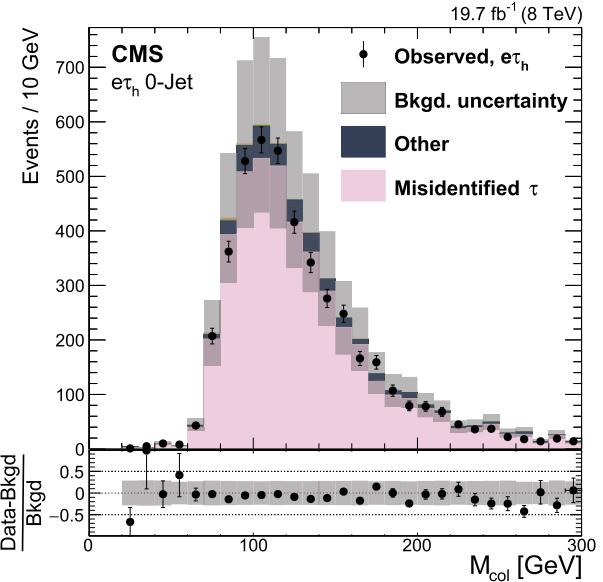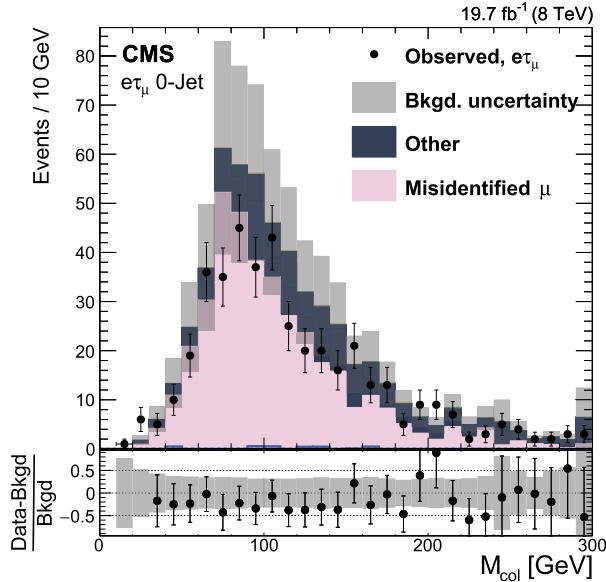

Fig. 2. Distributions of m_{col} for Region II. Left: $H \to e\tau_\mu$. Right: $H \to e\tau_h$.

Table 3

The systematic uncertainties in the expected event yields in percentage for the $e\tau_h$ and $e\tau_\mu$ channels. All uncertainties are treated as correlated between the categories, except when two values are quoted, in which case the number denoted by an asterisk is treated as uncorrelated between categories.

Systematic uncertainty	$H \to e\tau_\mu$			$H \to e\tau_h$		
	0-jet	1-jet	2-jet	0-jet	1-jet	2-jet
Muon trigger/ID/isolation	2	2	2	–	–	–
Electron trigger/ID/isolation	3	3	3	1	1	2
Efficiency of τ_h	–	–	–	6.7	6.7	6.7
$Z \to \tau\tau$ background	$3 \oplus 5^*$	$3 \oplus 5^*$	$3 \oplus 10^*$	$3 \oplus 5^*$	$3 \oplus 5^*$	$3 \oplus 10^*$
$Z \to \mu\mu$, ee background	30	30	30	30	30	30
Misidentified leptons background	40	40	40	30	30	30
Pileup	2	2	10	4	4	2
WW, WZ, ZZ + jets background	15	15	15	15	15	15
$t\bar{t}$ background	10	10	$10 \oplus 10^*$	10	10	$10 \oplus 33^*$
Single top quark background	25	25	25	25	25	25
b-tagging veto	3	3	3	–	–	–
Luminosity	2.6	2.6	2.6	2.6	2.6	2.6

Table 4

Theoretical uncertainties in percentage for the Higgs boson production cross section for each production process and category. All uncertainties are treated as fully correlated between categories except those denoted by a negative superscript which are fully anticorrelated due to the migration of events.

Systematic uncertainty	Gluon fusion			Vector boson fusion		
	0-jet	1-jet	2-jet	0-jet	1-jet	2-jet
Parton distribution function	9.7	9.7	9.7	3.6	3.6	3.6
Renormalization/factorization scale	8	10	30^-	4	1.5	2
Underlying event/parton shower	4	5^-	10^-	10	<1	1^-

derived from Region IV. The method assumes that the misidentification rate in $Z \to ee + X$ events is the same as in the $W + jets$ and QCD processes. To check this assumption, the misidentification rates are also measured in a collision data control sample of jets coming from QCD processes and found to be consistent. This sample is the same $Z \to ee + X$ sample as above but with one of the electron candidates required to be not isolated and the p_T threshold lowered.

5.2.3. Other backgrounds

The leptonic decay of W bosons from $t\bar{t}$ pairs produces opposite sign dileptons and E_T^{miss}. This background is estimated using simulated $t\bar{t}$ events to compute the M_{col} distribution and a collision data control region for normalization. The control region is the 2-jet selection described in Section 5.1, including the VBF requirements, with the additional requirement that at least one of the jets is b-tagged in order to enhance the $t\bar{t}$ contribution. Other smaller backgrounds enter from SM Higgs boson production ($H \to \tau\tau$), WW, WZ, ZZ + jets, $W\gamma^{(*)}$ + jets processes, and single top quark production. Each of these is estimated using simulation [38].

5.3. Systematic uncertainties

Systematic uncertainties are implemented as nuisance parameters in the signal and background fit to determine the scale of their effect. Some of these nuisance parameters affect only the background and signal normalizations, while others also affect the shape of the M_{col} distributions.

5.3.1. Normalization uncertainties

The values of the systematic uncertainties implemented as nuisance parameters in the signal and background fit are summarized in Tables 3 and 4. The uncertainties in the muon, electron and τ_h selection efficiencies (trigger, identification, and isolation) are estimated using collision data samples of $Z \to \mu\mu$, ee, $\tau_\mu\tau_h$ events [63,72]. The uncertainty in the $Z \to \tau\tau$ background yield

comes from the cross section uncertainty measurement (3% [73]) and from the uncertainty in the τ identification efficiency when applying to the embedded technique (5–10% uncorrelated between categories). The uncertainties in the estimation of the misidentified lepton rate come from the difference in rates measured in different collision data samples (QCD multijet and $W + jets$). The systematic uncertainty in the pileup modelling is evaluated by varying the total inelastic cross section by $\pm 5\%$ [74]. The uncertainties in the production cross sections estimated from simulation are also included [38].

Uncertainties on diboson and single top production correspond to the uncertainties of the respective cross section measurements [75,76]. A 10% uncertainty from the cross section measurement [77] is applied to the yield of the $t\bar{t}$ background. In the 2-jet categories an additional uncertainty (10% for $H \to e\tau_\mu$ and 33% for $H \to e\tau_h$) is considered corresponding to the statistical uncertainty of the $t\bar{t}$ background yield.

There are several theoretical uncertainties on the Higgs boson production cross section that depend on the production mechanism and the analysis category, as reported in Table 4. These uncertainties affect both the LFV Higgs boson and the SM Higgs boson background and are fully correlated. The uncertainty in the parton distribution function is evaluated by comparing the yields in each category, that span the parameter range of three different PDF sets, CT10 [47], MSTW [78], NNPDF [79] following the PDF4LHC [80] recommendation. The uncertainty due to the renormalization and factorization scales, μ_R and μ_F, is estimated by scaling up and down by a factor of two relative to their nominal values ($\mu_R = \mu_F = M_H/2$). The uncertainty in the simulation of the underlying event and parton showers is estimated by using two different PYTHIA tunes, AUET2 and Z2*. All uncertainties are treated as fully correlated between categories except those denoted by a negative superscript which are fully anticorrelated due to the migration of events.

Table 5
Systematic uncertainties in the shape of the signal and background distributions, expressed in percentage. The systematic uncertainty and its implementation are described in the text.

Systematic uncertainty	$H \to e\tau_\mu$	$H \to e\tau_h$
$Z \to \tau\tau$ bias	2	–
$Z \to ee$ bias	–	5
Jet energy scale	3–7	3–7
Jet energy resolution	1–10	1–10
Unclustered energy scale	10	10
τ_h energy scale	–	3

5.3.2. M_{col} shape uncertainties

The systematic uncertainties that lead to a change in the shape of the M_{col} distribution are summarized in Table 5. A 2% shift in the M_{col} distribution of the embedded $Z \to \tau\tau$ sample used to estimate the background is observed relative to simulation. It occurs only in the $H \to e\tau_\mu$ channel as the effects of bremsstrahlung from the muon are neglected in the simulation. The M_{col} distribution is corrected by $2 \pm 2\%$ for this effect. There is a systematic uncertainty of 5% in $Z \to ee$ background in the $H \to e\tau_h$ channel, due to the mismeasured energy of the electron reconstructed as a τ_h. It causes a shift in the M_{col} distribution, estimated by comparing collision data with simulation in a control region of $Z \to ee$ events in which one of the two electrons that form the Z peak is also identified as a τ_h [63]. Corrections are applied for the jet energy scale and resolution [66]. They are determined with dijet and $\gamma/Z +$ jets collision data and the most significant uncertainty arises from the photon energy scale. Other uncertainties such as jet fragmentation modelling, single pion response, and uncertainties in the pileup corrections are also included. The jet energy scale uncertainties (3–7%) are applied as a function of p_T and η, including all correlations, to all jets in the event, propagated to the E_T^{miss}, and the resultant M_{col} distribution is used in the fit. There is also an additional uncertainty to account for the unclustered energy scale uncertainty. The unclustered energy comes from jets below 10 GeV and PF candidates not within jets. It is also propagated to E_T^{miss}. These effects cause a shift of the M_{col} distribution. The uncertainty in the jet energy resolution is used to smear the jets as a function of p_T and η and the recomputed M_{col} distribution is used in the fit. A 3% uncertainty in the τ_h energy scale is estimated by comparing $Z \to \tau\tau$ events in collision data and simulation. Potential uncertainties in the shape of the misidentified lepton backgrounds are also considered. In the $H \to e\tau_\mu$ channel the misidentified lepton rates are applied in bins of p_T and η. In the $H \to e\tau_h$ channel, the τ_h misidentification rate is found to be approximately independent of p_T but to depend on η. These rates are all varied by one standard deviation and the differences in the shapes are used

as nuisance parameters in the fit. Finally, the distributions used in the fit have statistical uncertainties in each mass bin which is included as an uncertainty that is uncorrelated between the bins.

6. $H \to e\mu$ analysis

6.1. Event selection

To select $H \to e\mu$ events, the trigger requirement is an electron and a muon with p_T greater than 17 and 8 GeV respectively. To enhance the signal sensitivity the event sample is divided into nine different categories according to the region of detection of the leptons and the number of jets, and a further two categories enriched in vector boson fusion production. The resolution of the reconstructed mass of the electron muon system, $M_{e\mu}$, depends on whether the leptons are detected in the barrel ($|\eta_e| < 1.48$, $|\eta_\mu| < 0.80$) or endcap ($1.57 < |\eta_e| < 2.50$, $0.8 < |\eta_\mu| < 2.4$), while the composition and rate of backgrounds varies with the number of jets. The definition of the categories is shown in Table 6. The two leptons are required to be isolated in all categories. Categories 0–8, which are selected according to the region of detection of the lepton and number of jets, are mutually exclusive with jets required to have $p_T > 20$ GeV. To suppress backgrounds with significant E_T^{miss}, such as WW + jets, E_T^{miss} is required to be less than 20, 25 or 30 GeV, depending on the category. Jets arising from b quark decays are vetoed using the CSV discriminant to significantly reduce the t$\bar{\text{t}}$ background. In the VBF categories, the two highest p_T jets are required to have $|\eta| < 4.7$ and to be separated by $|\eta_{j_1} - \eta_{j_2}| > 3.0$. In addition the jets are required to have $|\eta^*| = |\eta_{\ell_1\ell_2} - \frac{\eta_{j_1} + \eta_{j_2}}{2}| < 2.5$, where $\ell = $ e or μ, $\eta_{\ell_1\ell_2}$ denotes the pseudorapidity of the dilepton system and j_1, j_2 are the two jets. The $\Delta\phi$ between the dijet system and the dilepton system is required to be greater than 2.6 rad. The VBF tight category selection further requires that both jets have $p_T > 30$ GeV and the dijet invariant mass be $M_{j_1j_2} > 500$ GeV, while the VBF loose category relaxes the second jet requirement to $p_T > 20$ GeV with $M_{j_1j_2} > 250$ GeV and is exclusive to the VBF tight category. The leptons in both VBF categories can be in either the barrel or endcap. To avoid an event appearing in more than one category the VBF assignment is made first. Events with more than two jets are not considered. The selection efficiency, summed over all categories, is 24% (22%) for the GF (VBF) production mechanism.

6.2. Signal and background modelling

The signal model is the sum of two Gaussian functions, determined from simulation for each category. The reconstructed

Table 6
The $H \to e\mu$ event selection criteria and background model for each event category. The categories are primarily defined according to whether the leptons are detected in the barrel (ℓ_B) or endcap (ℓ_{EC}), and the number of jets (N-jets). Requirements are also made on p_T^ℓ, E_T^{miss} and a veto on jets arising from a b-quark decay. The background model function and order of that function are also given.

Category	Description	N-jets	p_T^ℓ [GeV]	E_T^{miss} [GeV]	Background model Function	Order
0	$e_B\mu_B$	0	>25	<30	polynomial	4
1	$e_B\mu_B$	1	>22	<30	polynomial	4
2	$e_B\mu_B$	2	>25	<25	power law	1
3	$e_B\mu_{EC}$	0	>20	<30	polynomial	4
4	$e_B\mu_{EC}$	1	>22	<20	exponential	1
5	$e_B\mu_{EC}$	2	>20	<30	exponential	1
6	$e_{EC}\mu_{B \text{ or } EC}$	0	>20	<30	polynomial	4
7	$e_{EC}\mu_{B \text{ or } EC}$	1	>22	<20	power law	1
8	$e_{EC}\mu_{B \text{ or } EC}$	2	>20	<30	polynomial	4
9	VBF Tight	2	>22	<30	exponential	1
10	VBF Loose	2	>22	<25	exponential	1

mass resolutions depend on whether the leptons are in the barrel (B) or endcap (EC) calorimeter and are: 2.0–2.1 GeV for $e_B\mu_B$, 2.4–2.5 GeV for $e_B\mu_{EC}$, 3.2–3.6 GeV for $e_{EC}\mu_{B \text{ or } EC}$ categories and 2.4 (4.0) GeV for the VBF tight (loose) categories. The background, modelled as either a polynomial function, a sum of exponential functions, or a sum of power law functions is given in Table 6 for each category. The procedure to determine the background function follows the method described in [3]. It is designed to choose a model with sufficient parameters to accurately describe the background while ensuring that the signal shape is not absorbed into the background function. The background model for each category is chosen independently using this procedure.

In a first step, reference functions are selected for each type of function (polynomial, sum of exponentials, sum of power laws). The order of the function is chosen such that the next higher order does not give a significantly better fit result when fit to the observed $M_{e\mu}$ distribution in the range 110 GeV $< M_{e\mu} <$ 160 GeV.

In a second step, an ensemble of distributions is drawn from each of the three reference background models combined with a signal contribution corresponding to $\mathcal{B}(\text{H} \to e\mu) = 0.1\%$, and fitted for signal and background with each of the three classes of functions of different orders.

On average, the signal yield extracted from the distributions using a signal plus background fit will differ from the injected signal due to the imperfect modelling of the background. The bias is defined as the median deviation of the fit signal event yield from the generated number of signal events. The possible combinations of generated distributions with the fit signal plus background models are then reduced by requiring the bias to be less than a threshold which results in less than 1% uncertainty in the fit signal event yield. The combination in which the fit model has the least parameters is then selected and the fit function is used as the background model for the collision data. If there is more than one model with the same minimal number of parameters then the one with the least bias is selected.

6.3. Systematic uncertainties

The systematic uncertainties are summarized in Table 7. The background is fit to the observed mass distribution with a negligible systematic uncertainty of <1% in the signal yield arising from the choice of background model as described above. Correction factors are applied to the lepton trigger, isolation, and identification efficiencies for each simulated signal sample to adjust for discrepancies with the collision data. The uncertainty in the signal yield from the lepton isolation and identification corrections is 2.0% and is estimated with the "tag-and-probe" method [72] applied to a collision data sample of Z bosons decaying to lepton pairs [60,62]. The uncertainties in the lepton energy scale and the dilepton mass resolution are taken from the H $\to$ ZZ analysis [61]. The systematic uncertainty in the pileup modelling is evaluated by varying the total inelastic cross section by $\pm5\%$ [74]. It varies according to the production process and category between 0.7% and 2.3%. There are systematic uncertainties in the efficiency of the b quark jet veto that also vary with production process and category from 0.05% to 0.7%. The uncertainty on the integrated luminosity is 2.6% [81]. The effects of systematic uncertainties in the jet energy scale and resolution, and the uncertainties in PDF's on the selection efficiency are estimated as described in Section 5.3.2 for the H $\to$ eτ channel. The largest values of these systematic uncertainties occur due to the migration of events to, or from, a category with low statistics.

The theoretical uncertainties on the Higgs boson production cross section are also described in Section 5.3.2.

Table 7
Systematic uncertainties in percentage on the expected yield for H $\to$ eμ. Ranges are given where the uncertainty varies with production process and category. All uncertainties are treated as correlated between categories.

Experimental uncertainties	
Background model	<1
Trigger efficiency	1.0
Lepton identification	2.0
Lepton energy scale	1.0
Dilepton mass resolution	5.0
Pileup	0.7–2.3
b quark jet veto efficiency	0.05–0.70
Luminosity	2.6
Jet energy scale (inclusive categories)	0.6–22
Jet energy scale (VBF categories)	0.1–78
Jet energy resolution (inclusive categories)	2.8–12
Jet energy resolution (VBF categories)	0.0–49
Acceptance (PDF variations)	0.8–5.1
Theoretical uncertainties	
GF normalization/factorization scale	$^{+7.2}_{-7.8}$
GF parton distribution function	$^{+7.5}_{-6.9}$
VBF normalization/factorization scale	±0.2
VBF parton distribution function	$^{+2.6}_{-2.8}$

7. Results

7.1. H $\to$ eτ

The distributions of the fitted signal and background contributions, after the full selection, are shown in Fig. 3 and the corresponding event yields in the mass range 100 GeV $< M_{col} <$ 150 GeV are given in Table 8. There is no evidence of a signal. Table 9 shows the expected and observed 95% CL mean upper limits on $\mathcal{B}(\text{H} \to e\tau)$ which are summarized in Fig. 4 for the individual categories in the $e\tau_\mu$ and $e\tau_h$ channels and for the combination. The combined observed (expected) upper limit on $\mathcal{B}(\text{H} \to e\tau)$ is 0.69 (0.75)% at 95% CL [70,71,82].

7.2. H $\to$ eμ

The $M_{e\mu}$ distribution of the collision data sample, after all selection criteria, for all categories combined is shown in Fig. 5. Also shown are the combinations of the inclusive jet-tagged categories (0–8) and the VBF categories (9–10). The expected yields of signal ($\mathcal{B}(\text{H} \to e\mu) = 0.1\%$) and background events for 124 GeV $< M_{e\mu} <$ 126 GeV, after all the selection criteria, are given in Table 10 and compared to the collision data event yield. The contributions to the background are taken from simulation and given for information only, they are not used in the analysis. The dominant background contributions are from Drell–Yan production of τ lepton pairs and electroweak diboson production. There is no signal observed. An exclusion limit on the branching fraction $\mathcal{B}(\text{H} \to e\mu)$ with $M_H = 125$ GeV is derived using the CL_s asymptotic model [83]. It is shown in Fig. 4 for the inclusive categories grouped by number of jets, the VBF categories, and all categories combined. The expected limit is $\mathcal{B}(\text{H} \to e\mu) < 0.048\%$ at 95% CL and the observed limit is $\mathcal{B}(\text{H} \to e\mu) < 0.035\%$ at 95% CL.

7.3. Limits on lepton flavour violating couplings

The constraints on $\mathcal{B}(\text{H} \to e\tau)$ and $\mathcal{B}(\text{H} \to e\mu)$ can be interpreted in terms of the LFV Yukawa couplings $|Y_{e\tau}|$, $|Y_{\tau e}|$ and $|Y_{e\mu}|$, $|Y_{\mu e}|$ respectively [33]. The LFV decays H $\to$ eτ, eμ arise at tree level in the Lagrangian, L_V, from the flavour-violating Yukawa interactions, $Y_{\ell^\alpha \ell^\beta}$, where ℓ^α, ℓ^β denote the leptons e, μ, τ, and
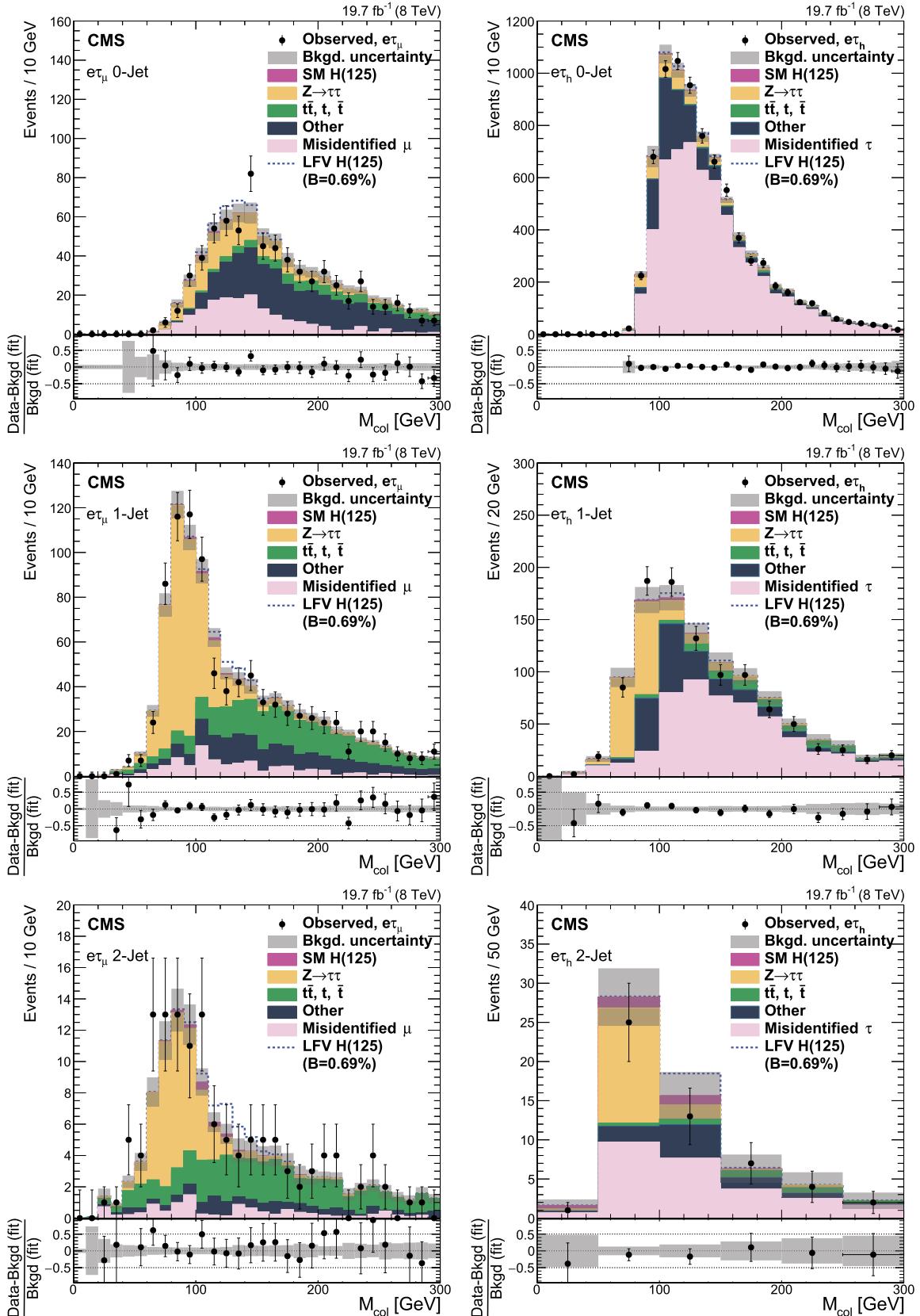
Fig. 3. Comparison of the observed collinear mass distributions with the background expectations after the fit. The simulated distributions for the signal are shown for the branching fraction $\mathcal{B}(H \to e\tau) = 0.69\%$. The left column is $H \to e\tau_\mu$ and the right column is $H \to e\tau_h$; the upper, middle and lower rows are the 0-jet, 1-jet and 2-jet categories, respectively.

Table 8

Event yields in the signal region, $100\text{ GeV} < M_{\text{col}} < 150\text{ GeV}$, after fitting for signal and background for the $\text{H} \to \text{e}\tau$ channel, normalized to an integrated luminosity of 19.7 fb^{-1}. The LFV Higgs boson signal is the expected yield for $\mathcal{B}(\text{H} \to \text{e}\tau) = 0.69\%$ assuming the SM Higgs boson production cross section.

Jet category	$\text{H} \to \text{e}\tau_\mu$			$\text{H} \to \text{e}\tau_h$		
	0-jet	1-jet	2-jet	0-jet	1-jet	2-jet
Misidentified leptons	85.2 ± 5.9	38.1 ± 3.9	2.1 ± 0.7	3366 ± 25	223 ± 11	8.7 ± 2.2
$Z \to \text{ee}, \mu\mu$	2.3 ± 0.6	5.4 ± 0.5	–	714 ± 30	85 ± 4	3.2 ± 0.2
$Z \to \tau\tau$	84.7 ± 2.1	113.3 ± 4.2	8.5 ± 0.6	270 ± 10	32 ± 3	1.6 ± 0.3
$\text{t}\bar{\text{t}}, \text{t}, \bar{\text{t}}$	13.8 ± 0.3	69.4 ± 2.3	12.7 ± 0.8	10 ± 2	13 ± 2	0.5 ± 0.2
ZZ, WZ, WW	83.0 ± 2.7	51.7 ± 2.0	3.6 ± 0.4	53 ± 2	6 ± 1	0.3 ± 0.1
$W\gamma(*)$	2.2 ± 1.0	1.2 ± 0.6	–	–	–	–
SM H background	2.3 ± 0.3	3.6 ± 0.4	1.1 ± 0.2	12 ± 1	3 ± 1	1.0 ± 0.1
Sum of background	273.5 ± 6.1	282.0 ± 6.0	28.1 ± 1.3	4425 ± 28	363 ± 11	15.3 ± 2.3
Observed	286	268	33	4438	375	13
LFV H signal	23.1 ± 1.6	16.0 ± 1.2	5.9 ± 1.0	61 ± 4	15 ± 1	2.8 ± 0.5
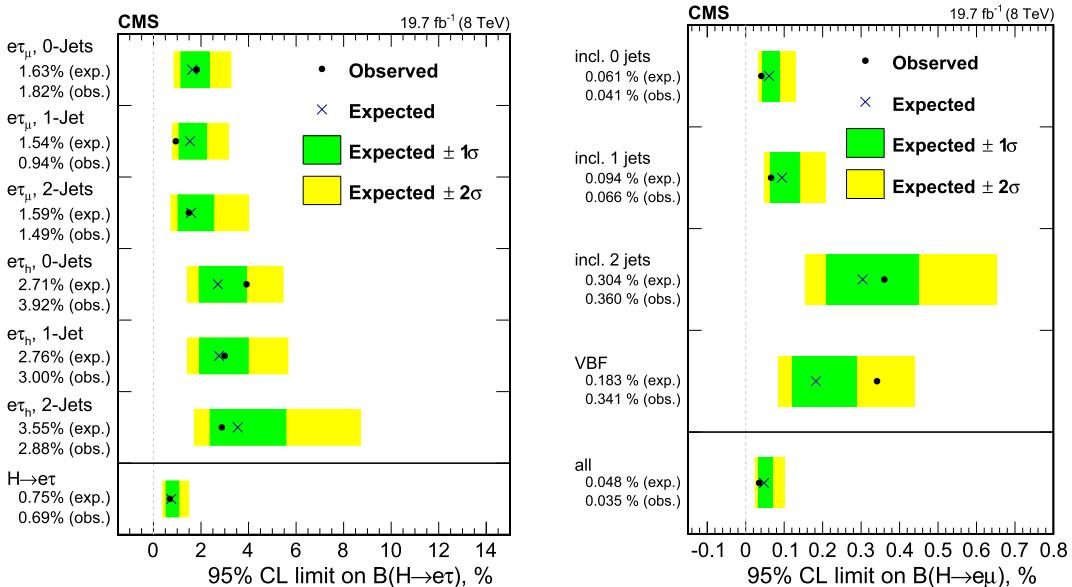
Fig. 4. 95% CL upper limits by category for the LFV decays for $M_\text{H} = 125\text{ GeV}$. Left: $\text{H} \to \text{e}\tau$. Right: $\text{H} \to \text{e}\mu$ for categories combined by number of jets, the VBF categories combined, and all categories combined.

Table 9

The expected and observed upper limits at 95% CL, and best fit values for the branching fractions $\mathcal{B}(\text{H} \to \text{e}\tau)$ for different jet categories and analysis channels. The asymmetric one standard-deviation uncertainties around the expected limits are shown in parentheses.

	0-jet	1-jet	2-jet
Expected limits at 95% CL (%)			
$\text{e}\tau_\mu$	$<1.63 \left({}^{+0.66}_{-0.44}\right)$	$<1.54 \left({}^{+0.71}_{-0.47}\right)$	$<1.59 \left({}^{+0.93}_{-0.55}\right)$
$\text{e}\tau_h$	$<2.71 \left({}^{+1.05}_{-0.75}\right)$	$<2.76 \left({}^{+1.07}_{-0.77}\right)$	$<3.55 \left({}^{+1.38}_{-0.99}\right)$
$\text{e}\tau$		$<0.75 \left({}^{+0.32}_{-0.22}\right)$	
Observed limits at 95% CL (%)			
$\text{e}\tau_\mu$	<1.83	<0.94	<1.49
$\text{e}\tau_h$	<3.92	<3.00	<2.88
$\text{e}\tau$		<0.69	

$\ell^\alpha \neq \ell^\beta$. The subscripts L and R refer to the left and right handed components of the leptons, respectively.

$$L_V \equiv -Y_{e\mu} \bar{e}_L \mu_R \text{H} - Y_{\mu e} \bar{\mu}_L e_R \text{H} - Y_{e\tau} \bar{e}_L \tau_R \text{H}$$
$$- Y_{\tau e} \bar{\tau}_L e_R \text{H} - Y_{\mu\tau} \bar{\mu}_L \tau_R \text{H} - Y_{\tau\mu} \bar{\tau}_L \mu_R \text{H}$$

The decay width $\Gamma(\text{H} \to \ell^\alpha \ell^\beta)$ in terms of the Yukawa couplings is given by:

Table 10

Event yields in the mass window $124\text{ GeV} < M_{\text{e}\mu} < 126\text{ GeV}$ for the $\text{H} \to \text{e}\mu$ channel. The expected contributions, estimated from simulation, are normalized to an integrated luminosity of 19.7 fb^{-1}. The LFV Higgs boson signal is the expectation for $\mathcal{B}(\text{H} \to \text{e}\mu) = 0.1\%$ assuming the SM production cross section. Values for background processes are given for information only and are not used for the analysis. The expected number of background events in the VBF categories obtained from simulation are associated with large uncertainties and are therefore not quoted here; we expect 1.5 ± 1.2 events from signal and observe 2 events.

Jet category	0-jet	1-jet	2-jet
Drell–Yan	17.8 ± 4.2	6.1 ± 2.5	1.9 ± 1.4
$\text{t}\bar{\text{t}}$	1.4 ± 1.2	3.1 ± 1.8	14.1 ± 3.8
$\text{t}, \bar{\text{t}}$	<1.0	<1.0	2.7 ± 1.6
WW, WZ, ZZ	21.6 ± 4.7	5.3 ± 2.3	1.9 ± 1.4
SM H background	<0.07	0.1 ± 0.2	<0.07
Sum of backgrounds	40.8 ± 6.4	14.6 ± 3.8	20.7 ± 4.5
Observed	49	6	17
LFV H signal	21.2 ± 4.6	9.1 ± 3.0	2.6 ± 1.6

$$\Gamma(\text{H} \to \ell^\alpha \ell^\beta) = \frac{M_\text{H}}{8\pi}(|Y_{\ell^\beta \ell^\alpha}|^2 + |Y_{\ell^\alpha \ell^\beta}|^2),$$

and the branching fraction by:

$$\mathcal{B}(\text{H} \to \ell^\alpha \ell^\beta) = \frac{\Gamma(\text{H} \to \ell^\alpha \ell^\beta)}{\Gamma(\text{H} \to \ell^\alpha \ell^\beta) + \Gamma_{\text{SM}}}.$$
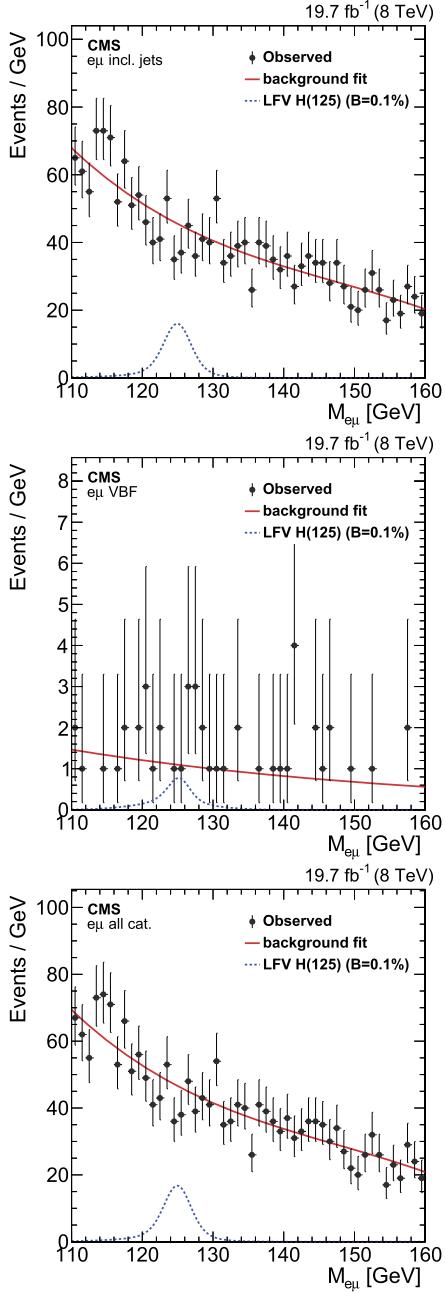
Fig. 5. Observed $e\mu$ mass spectra (points), background fit (solid line) and signal model (blue dashed line) for $\mathcal{B}(H \to e\mu) = 0.1\%$. Top: inclusive jet categories combined (0–8). Middle: VBF jet tagged categories combined (9–10). Bottom: all categories combined. (For interpretation of the references to colour in this figure legend, the reader is referred to the web version of this article.)

The SM Higgs boson decay width is $\Gamma_{\text{SM}} = 4.1$ MeV for a 125 GeV Higgs boson [84]. The 95% CL constraints on the Yukawa couplings, derived from $\mathcal{B}(H \to e\tau) < 0.69\%$ and $\mathcal{B}(H \to e\mu) < 0.035\%$ using the expression for the branching fraction above are:

$$\sqrt{|Y_{e\tau}|^2 + |Y_{\tau e}|^2} < 2.4 \times 10^{-3},$$

$$\sqrt{|Y_{e\mu}|^2 + |Y_{\mu e}|^2} < 5.4 \times 10^{-4}.$$

Figs. 6 compare these results to the constraints from previous indirect measurements. The absence of $\mu \to e\gamma$ decays implies a limit of $\sqrt{|Y_{e\mu}|^2 + |Y_{\mu e}|^2} < 3.6 \times 10^{-6}$ [33] assuming that flavour
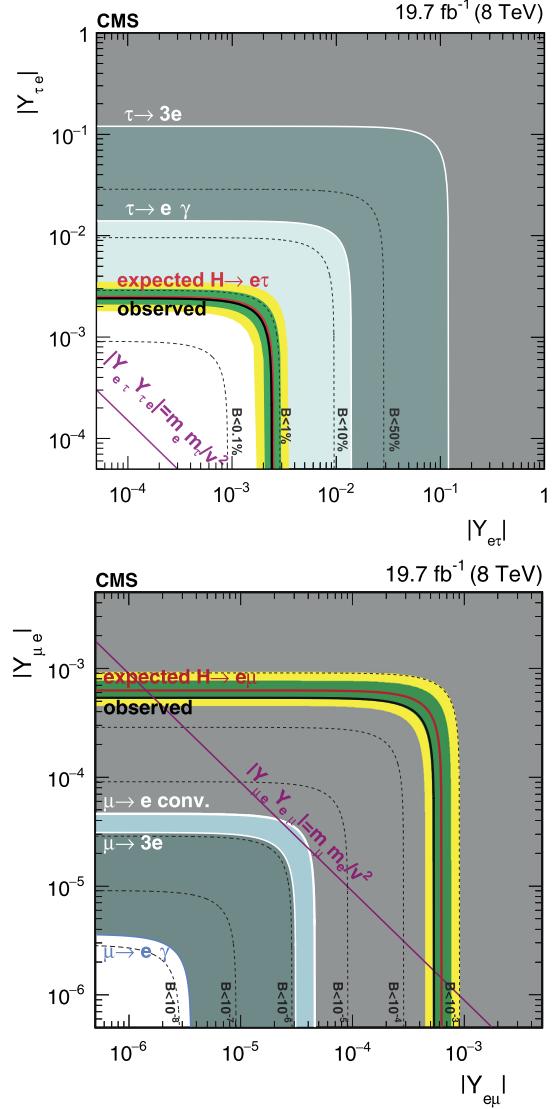
Fig. 6. Constraints on the flavour violating Yukawa couplings $|Y_{e\tau}|$, $|Y_{\tau e}|$ (top) and $|Y_{e\mu}|$, $|Y_{\mu e}|$ (bottom). The expected (red solid line) and observed (black solid line) limits are derived from the limits on $\mathcal{B}(H \to e\tau)$ and $\mathcal{B}(H \to e\mu)$ from the present analysis. The flavour diagonal Yukawa couplings are approximated by their SM values. The green (yellow) band indicates the range that is expected to contain 68% (95%) of all observed limit excursions. The shaded regions in the left plot are derived constraints from null searches for $\tau \to 3e$ (grey), $\tau \to e\gamma$ (dark green) and the present analysis (light blue). The shaded regions in the right plot are derived constraints from null searches for $\mu \to e\gamma$ (dark green), $\mu \to 3e$ (light blue) and $\mu \to e$ conversions (grey). The purple diagonal line is the theoretical naturalness limit $Y_{ij}Y_{ji} \leq m_i m_j / v^2$ [33]. (For interpretation of the references to colour in this figure legend, the reader is referred to the web version of this article.)

changing neutral currents are dominated by the Higgs boson contributions. However, this limit can be degraded by the cancellation of lepton flavour violating effects from other new physics. The direct search for $H \to e\mu$ decays presented here is therefore complementary to indirect limits obtained from searches for rare decays at lower energies.

8. Summary

A search for lepton flavour violating decays of the Higgs boson to $e\tau$ or $e\mu$, based on the full $\sqrt{s} = 8$ TeV collision data set collected by the CMS experiment in 2012, is presented. No evidence is found for such decays. Observed upper limits of $\mathcal{B}(H \to e\tau) < 0.69\%$ and $\mathcal{B}(H \to e\mu) < 0.035\%$ at 95% CL are set for

$M_H = 125$ GeV. These limits are used to constrain the $Y_{e\tau}$ and $Y_{e\mu}$ Yukawa couplings as follows: $\sqrt{|Y_{e\tau}|^2 + |Y_{\tau e}|^2} < 2.4 \times 10^{-3}$ and $\sqrt{|Y_{e\mu}|^2 + |Y_{\mu e}|^2} < 5.4 \times 10^{-4}$ at 95% CL.

References

[1] ATLAS Collaboration, Observation of a new particle in the search for the Standard Model Higgs boson with the ATLAS detector at the LHC, Phys. Lett. B 716 (2012) 1, http://dx.doi.org/10.1016/j.physletb.2012.08.020, arXiv:1207.7214.

[2] CMS Collaboration, Observation of a new boson at a mass of 125 GeV with the CMS experiment at the LHC, Phys. Lett. B 716 (2012) 30, http://dx.doi.org/10.1016/j.physletb.2012.08.021, arXiv:1207.7235.

[3] CMS Collaboration, Observation of a new boson with mass near 125 GeV in pp collisions at $\sqrt{s} = 7$ and 8 TeV, J. High Energy Phys. 06 (2013) 081, http://dx.doi.org/10.1007/JHEP06(2013)081, arXiv:1303.4571.

[4] J.D. Bjorken, S. Weinberg, Mechanism for nonconservation of muon number, Phys. Rev. Lett. 38 (1977) 622, http://dx.doi.org/10.1103/PhysRevLett.38.622.

[5] J.L. Diaz-Cruz, J.J. Toscano, Lepton flavor violating decays of Higgs bosons beyond the standard model, Phys. Rev. D 62 (2000) 116005, http://dx.doi.org/10.1103/PhysRevD.62.116005, arXiv:hep-ph/9910233.

[6] T. Han, D. Marfatia, $h \to \mu\tau$ at hadron colliders, Phys. Rev. Lett. 86 (2001) 1442, http://dx.doi.org/10.1103/PhysRevLett.86.1442, arXiv:hep-ph/0008141.

[7] E. Arganda, A.M. Curiel, M.J. Herrero, D. Temes, Lepton flavor violating Higgs boson decays from massive seesaw neutrinos, Phys. Rev. D 71 (2005) 035011, http://dx.doi.org/10.1103/PhysRevD.71.035011, arXiv:hep-ph/0407302.

[8] A. Arhrib, Y. Cheng, O.C.W. Kong, Comprehensive analysis on lepton flavor violating Higgs boson to $\mu\bar{\tau} + \tau\bar{\mu}$ decay in supersymmetry without R parity, Phys. Rev. D 87 (2013) 015025, http://dx.doi.org/10.1103/PhysRevD.87.015025, arXiv:1210.8241.

[9] M. Arana-Catania, E. Arganda, M.J. Herrero, Non-decoupling SUSY in LFV Higgs decays: a window to new physics at the LHC, J. High Energy Phys. 09 (2013) 160, http://dx.doi.org/10.1007/JHEP09(2013)160, arXiv:1304.3371, Erratum: http://dx.doi.org/10.1007/JHEP10(2015)192.

[10] E. Arganda, M.J. Herrero, R. Morales, A. Szynkman, Analysis of the $h, H, A \to \tau\mu$ decays induced from SUSY loops within the mass insertion approximation, J. High Energy Phys. 03 (2016) 055, http://dx.doi.org/10.1007/JHEP03(2016)055, arXiv:1510.04685.

[11] E. Arganda, M.J. Herrero, X. Marcano, C. Weiland, Enhancement of the lepton flavor violating Higgs boson decay rates from SUSY loops in the inverse seesaw model, Phys. Rev. D 93 (2016) 055010, http://dx.doi.org/10.1103/PhysRevD.93.055010, arXiv:1508.04623.

[12] K. Agashe, R. Contino, Composite Higgs-mediated flavor-changing neutral current, Phys. Rev. D 80 (2009) 075016, http://dx.doi.org/10.1103/PhysRevD.80.075016, arXiv:0906.1542.

[13] A. Azatov, M. Toharia, L. Zhu, Higgs mediated flavor changing neutral currents in warped extra dimensions, Phys. Rev. D 80 (2009) 035016, http://dx.doi.org/10.1103/PhysRevD.80.035016, arXiv:0906.1990.

[14] H. Ishimori, T. Kobayashi, H. Ohki, Y. Shimizu, H. Okada, M. Tanimoto, Non-Abelian discrete symmetries in particle physics, Prog. Theor. Phys. Suppl. 183 (2010) 1, http://dx.doi.org/10.1143/PTPS.183.1, arXiv:1003.3552.

[15] G. Perez, L. Randall, Natural neutrino masses and mixings from warped geometry, J. High Energy Phys. 01 (2009) 077, http://dx.doi.org/10.1088/1126-6708/2009/01/077, arXiv:0805.4652.

[16] S. Casagrande, F. Goertz, U. Haisch, M. Neubert, T. Pfoh, Flavor physics in the Randall–Sundrum model I. Theoretical setup and electroweak precision tests, J. High Energy Phys. 10 (2008) 094, http://dx.doi.org/10.1088/1126-6708/2008/10/094, arXiv:0807.4937.

[17] A.J. Buras, B. Duling, S. Gori, The impact of Kaluza–Klein fermions on Standard Model fermion couplings in a RS model with custodial protection, J. High Energy Phys. 09 (2009) 076, http://dx.doi.org/10.1088/1126-6708/2009/09/076, arXiv:0905.2318.

[18] M. Blanke, A.J. Buras, B. Duling, S. Gori, A. Weiler, $\Delta F = 2$ observables and fine-tuning in a warped extra dimension with custodial protection, J. High Energy Phys. 03 (2009) 001, http://dx.doi.org/10.1088/1126-6708/2009/03/001, arXiv:0809.1073.

[19] G.F. Giudice, O. Lebedev, Higgs-dependent Yukawa couplings, Phys. Lett. B 665 (2008) 79, http://dx.doi.org/10.1016/j.physletb.2008.05.062, arXiv:0804.1753.

[20] J.A. Aguilar-Saavedra, A minimal set of top-Higgs anomalous couplings, Nucl. Phys. B 821 (2009) 215, http://dx.doi.org/10.1016/j.nuclphysb.2009.06.022, arXiv:0904.2387.

[21] M.E. Albrecht, M. Blanke, A.J. Buras, B. Duling, K. Gemmler, Electroweak and flavour structure of a warped extra dimension with custodial protection, J. High Energy Phys. 09 (2009) 064, http://dx.doi.org/10.1088/1126-6708/2009/09/064, arXiv:0903.2415.

[22] A. Goudelis, O. Lebedev, J.H. Park, Higgs-induced lepton flavor violation, Phys. Lett. B 707 (2012) 369, http://dx.doi.org/10.1016/j.physletb.2011.12.059, arXiv:1111.1715.

[23] D. McKeen, M. Pospelov, A. Ritz, Modified Higgs branching ratios versus CP and lepton flavor violation, Phys. Rev. D 86 (2012) 113004, http://dx.doi.org/10.1103/PhysRevD.86.113004, arXiv:1208.4597.

[24] A. Pilaftsis, Lepton flavour nonconservation in H^0 decays, Phys. Lett. B 285 (1992) 68, http://dx.doi.org/10.1016/0370-2693(92)91301-O.

[25] J.G. Körner, A. Pilaftsis, K. Schilcher, Leptonic CP asymmetries in flavor-changing H^0 decays, Phys. Rev. D 47 (1993) 1080, http://dx.doi.org/10.1103/PhysRevD.47.1080.

[26] E. Arganda, M.J. Herrero, X. Marcano, C. Weiland, Imprints of massive inverse seesaw model neutrinos in lepton flavor violating Higgs boson decays, Phys. Rev. D 91 (2015) 015001, http://dx.doi.org/10.1103/PhysRevD.91.015001, arXiv:1405.4300.

[27] CMS Collaboration, Search for lepton-flavour-violating decays of the Higgs boson, Phys. Lett. B 749 (2015) 337, http://dx.doi.org/10.1016/j.physletb.2015.07.053, arXiv:1502.07400.

[28] ATLAS Collaboration, Search for lepton-flavour-violating $H \to \mu\tau$ decays of the Higgs boson with the ATLAS detector, J. High Energy Phys. 11 (2015) 211, http://dx.doi.org/10.1007/JHEP11(2015)211, arXiv:1508.03372.

[29] ATLAS Collaboration, Search for lepton-flavour-violating decays of the Higgs and Z bosons with the ATLAS detector, arXiv:1604.07730, 2016, J. High Energy Phys., submitted for publication.

[30] B. McWilliams, L.-F. Li, Virtual effects of Higgs particles, Nucl. Phys. B 179 (1981) 62, http://dx.doi.org/10.1016/0550-3213(81)90249-2.

[31] O.U. Shanker, Flavour violation, scalar particles and leptoquarks, Nucl. Phys. B 206 (1982) 253, http://dx.doi.org/10.1016/0550-3213(82)90534-X.

[32] G. Blankenburg, J. Ellis, G. Isidori, Flavour-changing decays of a 125 GeV Higgs-like particle, Phys. Lett. B 712 (2012) 386, http://dx.doi.org/10.1016/j.physletb.2012.05.007, arXiv:1202.5704.

[33] R. Harnik, J. Kopp, J. Zupan, Flavor violating Higgs decays, J. High Energy Phys. 03 (2013) 26, http://dx.doi.org/10.1007/JHEP03(2013)026, arXiv:1209.1397.

[34] Particle Data Group, J. Beringer, et al., in: Review of Particle Physics, Phys. Rev. D 86 (2012) 010001, http://dx.doi.org/10.1103/PhysRevD.86.010001.

[35] A. Celis, V. Cirigliano, E. Passemar, Lepton flavor violation in the Higgs sector and the role of hadronic tau-lepton decays, Phys. Rev. D 89 (2014) 013008, http://dx.doi.org/10.1103/PhysRevD.89.013008, arXiv:1309.3564.

[36] S.M. Barr, A. Zee, Electric dipole moment of the electron and of the neutron, Phys. Rev. Lett. 65 (1990) 21, http://dx.doi.org/10.1103/PhysRevLett.65.21.

[37] CMS Collaboration, Evidence for the direct decay of the 125 GeV Higgs boson to fermions, Nat. Phys. 10 (2014) 557, http://dx.doi.org/10.1038/nphys3005, arXiv:1401.6527.

[38] CMS Collaboration, Evidence for the 125 GeV Higgs boson decaying to a pair of τ leptons, J. High Energy Phys. 05 (2014) 104, http://dx.doi.org/10.1007/JHEP05(2014)104, arXiv:1401.5041.

[39] ATLAS Collaboration, Evidence for the Higgs-boson Yukawa coupling to tau leptons with the ATLAS detector, J. High Energy Phys. 04 (2015) 117, http://dx.doi.org/10.1007/JHEP04(2015)117, arXiv:1501.04943.

[40] CMS Collaboration, The CMS experiment at the CERN LHC, J. Instrum. 3 (2008) S08004, http://dx.doi.org/10.1088/1748-0221/3/08/S08004.

[41] S. Agostinelli, et al., GEANT4 Collaboration, GEANT4 – a simulation toolkit, Nucl. Instrum. Methods Phys. Res., Sect. A 506 (2003) 250, http://dx.doi.org/10.1016/S0168-9002(03)01368-8.

[42] H.M. Georgi, S.L. Glashow, M.E. Machacek, D.V. Nanopoulos, Higgs bosons from two gluon annihilation in proton proton collisions, Phys. Rev. Lett. 40 (1978) 692, http://dx.doi.org/10.1103/PhysRevLett.40.692.

[43] R.N. Cahn, S.D. Ellis, R. Kleiss, W.J. Stirling, Transverse-momentum signatures for heavy Higgs bosons, Phys. Rev. D 35 (1987) 1626, http://dx.doi.org/10.1103/PhysRevD.35.1626.

[44] S.L. Glashow, D.V. Nanopoulos, A. Yildiz, Associated production of Higgs bosons and Z particles, Phys. Rev. D 18 (1978) 1724, http://dx.doi.org/10.1103/PhysRevD.18.1724.

[45] T. Sjöstrand, S. Mrenna, P. Skands, A brief introduction to PYTHIA 8.1, Comput. Phys. Commun. 178 (2007) 852, http://dx.doi.org/10.1016/j.cpc.2008.01.036, arXiv:0710.3820.

[46] T. Sjöstrand, S. Mrenna, P. Skands, PYTHIA 6.4 physics and manual, J. High Energy Phys. 05 (2006) 026, http://dx.doi.org/10.1088/1126-6708/2006/05/026, arXiv:hep-ph/0603175.

[47] P.M. Nadolsky, H.-L. Lai, Q.-H. Cao, J. Huston, J. Pumplin, D. Stump, W.-K. Tung, C.-P. Yuan, Implications of CTEQ global analysis for collider observables, Phys. Rev. D 78 (2008) 013004, http://dx.doi.org/10.1103/PhysRevD.78.013004, arXiv:0802.0007.

[48] P. Nason, A new method for combining NLO QCD with shower Monte Carlo algorithms, J. High Energy Phys. 11 (2004) 040, http://dx.doi.org/10.1088/1126-6708/2004/11/040, arXiv:hep-ph/0409146.

[49] S. Frixione, P. Nason, C. Oleari, Matching NLO QCD computations with parton shower simulations: the POWHEG method, J. High Energy Phys. 11 (2007) 070, http://dx.doi.org/10.1088/1126-6708/2007/11/070, arXiv:0709.2092.

[50] S. Alioli, P. Nason, C. Oleari, E. Re, A general framework for implementing NLO calculations in shower Monte Carlo programs: the POWHEG BOX, J. High Energy Phys. 06 (2010) 043, http://dx.doi.org/10.1007/JHEP06(2010)043, arXiv:1002.2581.

[51] S. Alioli, K. Hamilton, P. Nason, C. Oleari, E. Re, Jet pair production in POWHEG, J. High Energy Phys. 04 (2011) 081, http://dx.doi.org/10.1007/JHEP04(2011)081, arXiv:1012.3380.

[52] S. Alioli, P. Nason, C. Oleari, E. Re, NLO Higgs boson production via gluon fusion matched with shower in POWHEG, J. High Energy Phys. 04 (2009) 002, http://dx.doi.org/10.1088/1126-6708/2009/04/002, arXiv:0812.0578.

[53] J. Alwall, M. Herquet, F. Maltoni, O. Mattelaer, T. Stelzer, MadGraph 5: going beyond, J. High Energy Phys. 06 (2011) 128, http://dx.doi.org/10.1007/JHEP06(2011)128, arXiv:1106.0522.

[54] R. Field, Early LHC underlying event data – findings and surprises, in: Proceedings of the 22nd Conference on Hadron Collider Physics, HCP 2010, Toronto, Canada, 23–27 August 2010, 2010, arXiv:1010.3558.

[55] CMS Collaboration, Description and performance of track and primary-vertex reconstruction with the CMS tracker, J. Instrum. 9 (2014) P10009, http://dx.doi.org/10.1088/1748-0221/9/10/P10009, arXiv:1405.6569.

[56] CMS Collaboration, Particle-Flow Event Reconstruction in CMS and Performance for Jets, Taus, and $E_{\mathrm{T}}^{\mathrm{miss}}$, CMS Physics Analysis Summary CMS-PAS-PFT-09-001, 2009, http://cdsweb.cern.ch/record/1194487.

[57] CMS Collaboration, Particle Flow Reconstruction of 0.9 TeV and 2.36 TeV collision Events in CMS, CMS Physics Analysis Note CMS-PAS-PFT-10-001, 2010, http://cds.cern.ch/record/1247373.

[58] CMS Collaboration, Commissioning of the Particle-Flow Event Reconstruction with Leptons from J/ψ and W Decays at 7 TeV, CMS Physics Analysis Summary CMS-PAS-PFT-10-003, 2010, http://cdsweb.cern.ch/record/1279347.

[59] CMS Collaboration, Performance of the CMS missing transverse momentum reconstruction in pp data at $\sqrt{s} =$ 8 TeV, J. Instrum. 10 (2015) P02006, http://dx.doi.org/10.1088/1748-0221/10/02/P02006, arXiv:1411.0511.

[60] CMS Collaboration, Performance of electron reconstruction and selection with the CMS detector in proton–proton collisions at $\sqrt{s} =$ 8 TeV, J. Instrum. 10 (2015) P06005, http://dx.doi.org/10.1088/1748-0221/10/06/P06005, arXiv:1502.02701.

[61] CMS Collaboration, Measurement of the properties of a Higgs boson in the four-lepton final state, Phys. Rev. D 89 (2014) 092007, http://dx.doi.org/10.1103/PhysRevD.89.092007, arXiv:1312.5353.

[62] CMS Collaboration, Performance of CMS muon reconstruction in pp collision events at $\sqrt{s} =$ 7 TeV, J. Instrum. 7 (2012) P10002, http://dx.doi.org/10.1088/1748-0221/7/10/P10002, arXiv:1206.4071.

[63] CMS Collaboration, Reconstruction and identification of tau lepton decays to hadrons and ν_τ at CMS, J. Instrum. 11 (2016) P01019, http://dx.doi.org/10.1088/1748-0221/11/01/P01019, arXiv:1510.07488.

[64] M. Cacciari, G.P. Salam, G. Soyez, FastJet user manual, Eur. Phys. J. C 72 (2012) 1896, http://dx.doi.org/10.1140/epjc/s10052-012-1896-2, arXiv:1111.6097.

[65] M. Cacciari, G.P. Salam, G. Soyez, The anti-k_t jet clustering algorithm, J. High Energy Phys. 04 (2008) 063, http://dx.doi.org/10.1088/1126-6708/2008/04/063, arXiv:0802.1189.

[66] CMS Collaboration, Determination of jet energy calibration and transverse momentum resolution in CMS, J. Instrum. 6 (2011) 11002, http://dx.doi.org/10.1088/1748-0221/6/11/P11002, arXiv:1107.4277.

[67] CMS Collaboration, Pile-up Jet Identification, CMS Physics Analysis Summary CMS-PAS-JME-13-005, 2013, http://cdsweb.cern.ch/record/1581583.

[68] R.K. Ellis, I. Hinchliffe, M. Soldate, J.J. van der Bij, Higgs decay to $\tau^+\tau^-$: a possible signature of intermediate mass Higgs bosons at high energy hadron colliders, Nucl. Phys. B 297 (1988) 221, http://dx.doi.org/10.1016/0550-3213(88)90019-3.

[69] CMS Collaboration, Performance of b Tagging at $\sqrt{s} =$ 8 TeV in Multijet, t$\bar{\mathrm{t}}$ and Boosted Topology Events, CMS Physics Analysis Summary CMS-PAS-BTV-13-001, 2013, https://cds.cern.ch/record/1581306.

[70] T. Junk, Confidence level computation for combining searches with small statistics, Nucl. Instrum. Methods Phys. Res., Sect. A 434 (1999) 435, http://dx.doi.org/10.1016/S0168-9002(99)00498-2, arXiv:hep-ex/9902006.

[71] A.L. Read, Presentation of search results: the CL_s technique, J. Phys. G 28 (2002) 2693, http://dx.doi.org/10.1088/0954-3899/28/10/313.

[72] CMS Collaboration, Measurement of the inclusive W and Z production cross sections in pp collisions at $\sqrt{s} =$ 7 TeV with the CMS experiment, J. High Energy Phys. 10 (2011) 132, http://dx.doi.org/10.1007/JHEP10(2011)132, arXiv:1107.4789.

[73] CMS Collaboration, Measurement of inclusive W and Z boson production cross sections in pp collisions at $\sqrt{s} =$ 8 TeV, Phys. Rev. Lett. 112 (2014) 191802, http://dx.doi.org/10.1103/PhysRevLett.112.191802, arXiv:1402.0923.

[74] CMS Collaboration, Measurement of the inelastic proton–proton cross section at $\sqrt{s} =$ 7 TeV, Phys. Lett. B 722 (2013) 5, http://dx.doi.org/10.1016/j.physletb.2013.03.024.

[75] CMS Collaboration, Measurement of the W$^+$W$^-$ and ZZ production cross sections in pp collisions at $\sqrt{s} =$ 8 TeV, Phys. Lett. B 721 (2013) 190, http://dx.doi.org/10.1016/j.physletb.2013.03.027, arXiv:1301.4698.

[76] CMS Collaboration, Observation of the associated production of a single top quark and a W boson in pp collisions at $\sqrt{s} =$ 8 TeV, Phys. Rev. Lett. 112 (2014) 231802, http://dx.doi.org/10.1103/PhysRevLett.112.231802, arXiv:1401.2942.

[77] CMS Collaboration, Measurement of the t$\bar{\mathrm{t}}$ production cross section in pp collisions at $\sqrt{s} =$ 8 TeV in dilepton final states containing one τ lepton, Phys. Lett. B 739 (2014) 23, http://dx.doi.org/10.1016/j.physletb.2014.10.032, arXiv:1407.6643.

[78] A.D. Martin, W.J. Stirling, R.S. Thorne, G. Watt, Parton distributions for the LHC, Eur. Phys. J. C 63 (2009) 189, http://dx.doi.org/10.1140/epjc/s10052-009-1072-5, arXiv:0901.0002.

[79] R.D. Ball, L. Del Debbio, S. Forte, A. Guffanti, J.I. Latorre, J. Rojo, M. Ubiali (NNPDF), A first unbiased global NLO determination of parton distributions and their uncertainties, Nucl. Phys. B 838 (2010) 136, http://dx.doi.org/10.1016/j.nuclphysb.2010.05.008, arXiv:1002.4407.

[80] M. Botje, J. Butterworth, A. Cooper-Sarkar, A. de Roeck, J. Feltesse, S. Forte, A. Glazov, J. Huston, R. McNulty, T. Sjöstrand, R.S. Thorne, The PDF4LHC working group interim recommendations, arXiv:1101.0538, 2011.

[81] CMS Collaboration, CMS Luminosity Based on Pixel Cluster Counting – Summer 2013 Update, CMS Physics Analysis Summary CMS-PAS-LUM-13-001, 2013, http://cds.cern.ch/record/1598864.

[82] Procedure for the LHC Higgs Boson Search Combination in Summer 2011, Technical report ATL-PHYS-PUB-2011-011, ATL-COM-PHYS-2011-818, CMS-NOTE-2011-005, 2011, https://cds.cern.ch/record/1375842.

[83] G. Cowan, K. Cranmer, E. Gross, O. Vitells, Asymptotic formulae for likelihood-based tests of new physics, Eur. Phys. J. C 71 (2011) 1554, http://dx.doi.org/10.1140/epjc/s10052-011-1554-0, arXiv:1007.1727.

[84] A. Denner, S. Heinemeyer, I. Puljak, D. Rebuzzi, M. Spira, Standard model Higgs-boson branching ratios with uncertainties, Eur. Phys. J. C 71 (2011) 1753, http://dx.doi.org/10.1140/epjc/s10052-011-1753-8, arXiv:1107.5909.

The CMS Collaboration

V. Khachatryan, A.M. Sirunyan, A. Tumasyan

Yerevan Physics Institute, Yerevan, Armenia

W. Adam, E. Asilar, T. Bergauer, J. Brandstetter, E. Brondolin, M. Dragicevic, J. Erö, M. Flechl, M. Friedl, R. Frühwirth [1], V.M. Ghete, C. Hartl, N. Hörmann, J. Hrubec, M. Jeitler [1], V. Knünz, A. König, M. Krammer [1], I. Krätschmer, D. Liko, T. Matsushita, I. Mikulec, D. Rabady [2], B. Rahbaran, H. Rohringer, J. Schieck [1], R. Schöfbeck, J. Strauss, W. Treberer-Treberspurg, W. Waltenberger, C.-E. Wulz [1]

Institut für Hochenergiephysik der OeAW, Wien, Austria

V. Mossolov, N. Shumeiko, J. Suarez Gonzalez

National Centre for Particle and High Energy Physics, Minsk, Belarus

S. Alderweireldt, T. Cornelis, E.A. De Wolf, X. Janssen, A. Knutsson, J. Lauwers, S. Luyckx, M. Van De Klundert, H. Van Haevermaet, P. Van Mechelen, N. Van Remortel, A. Van Spilbeeck

Universiteit Antwerpen, Antwerpen, Belgium

S. Abu Zeid, F. Blekman, J. D'Hondt, N. Daci, I. De Bruyn, K. Deroover, N. Heracleous, J. Keaveney, S. Lowette, L. Moreels, A. Olbrechts, Q. Python, D. Strom, S. Tavernier, W. Van Doninck, P. Van Mulders, G.P. Van Onsem, I. Van Parijs

Vrije Universiteit Brussel, Brussel, Belgium

P. Barria, H. Brun, C. Caillol, B. Clerbaux, G. De Lentdecker, G. Fasanella, L. Favart, A. Grebenyuk, G. Karapostoli, T. Lenzi, A. Léonard, T. Maerschalk, A. Marinov, L. Perniè, A. Randle-conde, T. Seva, C. Vander Velde, P. Vanlaer, R. Yonamine, F. Zenoni, F. Zhang [3]

Université Libre de Bruxelles, Bruxelles, Belgium

K. Beernaert, L. Benucci, A. Cimmino, S. Crucy, D. Dobur, A. Fagot, G. Garcia, M. Gul, J. Mccartin, A.A. Ocampo Rios, D. Poyraz, D. Ryckbosch, S. Salva, M. Sigamani, M. Tytgat, W. Van Driessche, E. Yazgan, N. Zaganidis

Ghent University, Ghent, Belgium

S. Basegmez, C. Beluffi [4], O. Bondu, S. Brochet, G. Bruno, A. Caudron, L. Ceard, G.G. Da Silveira, C. Delaere, D. Favart, L. Forthomme, A. Giammanco [5], J. Hollar, A. Jafari, P. Jez, M. Komm, V. Lemaitre, A. Mertens, M. Musich, C. Nuttens, L. Perrini, A. Pin, K. Piotrzkowski, A. Popov [6], L. Quertenmont, M. Selvaggi, M. Vidal Marono

Université Catholique de Louvain, Louvain-la-Neuve, Belgium

N. Beliy, G.H. Hammad

Université de Mons, Mons, Belgium

W.L. Aldá Júnior, F.L. Alves, G.A. Alves, L. Brito, M. Correa Martins Junior, M. Hamer, C. Hensel, A. Moraes, M.E. Pol, P. Rebello Teles

Centro Brasileiro de Pesquisas Fisicas, Rio de Janeiro, Brazil

E. Belchior Batista Das Chagas, W. Carvalho, J. Chinellato [7], A. Custódio, E.M. Da Costa,
D. De Jesus Damiao, C. De Oliveira Martins, S. Fonseca De Souza, L.M. Huertas Guativa, H. Malbouisson,
D. Matos Figueiredo, C. Mora Herrera, L. Mundim, H. Nogima, W.L. Prado Da Silva, A. Santoro,
A. Sznajder, E.J. Tonelli Manganote [7], A. Vilela Pereira

Universidade do Estado do Rio de Janeiro, Rio de Janeiro, Brazil

S. Ahuja [a], C.A. Bernardes [b], A. De Souza Santos [b], S. Dogra [a], T.R. Fernandez Perez Tomei [a],
E.M. Gregores [b], P.G. Mercadante [b], C.S. Moon [a,8], S.F. Novaes [a], Sandra S. Padula [a], D. Romero Abad,
J.C. Ruiz Vargas

[a] *Universidade Estadual Paulista, São Paulo, Brazil*
[b] *Universidade Federal do ABC, São Paulo, Brazil*

A. Aleksandrov, R. Hadjiiska, P. Iaydjiev, M. Rodozov, S. Stoykova, G. Sultanov, M. Vutova

Institute for Nuclear Research and Nuclear Energy, Sofia, Bulgaria

A. Dimitrov, I. Glushkov, L. Litov, B. Pavlov, P. Petkov

University of Sofia, Sofia, Bulgaria

M. Ahmad, J.G. Bian, G.M. Chen, H.S. Chen, M. Chen, T. Cheng, R. Du, C.H. Jiang, R. Plestina [9], F. Romeo,
S.M. Shaheen, A. Spiezia, J. Tao, C. Wang, Z. Wang, H. Zhang

Institute of High Energy Physics, Beijing, China

C. Asawatangtrakuldee, Y. Ban, Q. Li, S. Liu, Y. Mao, S.J. Qian, D. Wang, Z. Xu

State Key Laboratory of Nuclear Physics and Technology, Peking University, Beijing, China

C. Avila, A. Cabrera, L.F. Chaparro Sierra, C. Florez, J.P. Gomez, B. Gomez Moreno, J.C. Sanabria

Universidad de Los Andes, Bogota, Colombia

N. Godinovic, D. Lelas, I. Puljak, P.M. Ribeiro Cipriano

University of Split, Faculty of Electrical Engineering, Mechanical Engineering and Naval Architecture, Split, Croatia

Z. Antunovic, M. Kovac

University of Split, Faculty of Science, Split, Croatia

V. Brigljevic, K. Kadija, J. Luetic, S. Micanovic, L. Sudic

Institute Rudjer Boskovic, Zagreb, Croatia

A. Attikis, G. Mavromanolakis, J. Mousa, C. Nicolaou, F. Ptochos, P.A. Razis, H. Rykaczewski

University of Cyprus, Nicosia, Cyprus

M. Bodlak, M. Finger [10], M. Finger Jr. [10]

Charles University, Prague, Czech Republic

A.A. Abdelalim [11,12], A. Awad, A. Mahrous [11], A. Radi [13,14]

Academy of Scientific Research and Technology of the Arab Republic of Egypt, Egyptian Network of High Energy Physics, Cairo, Egypt

B. Calpas, M. Kadastik, M. Murumaa, M. Raidal, A. Tiko, C. Veelken

National Institute of Chemical Physics and Biophysics, Tallinn, Estonia

P. Eerola, J. Pekkanen, M. Voutilainen

Department of Physics, University of Helsinki, Helsinki, Finland

J. Härkönen, V. Karimäki, R. Kinnunen, T. Lampén, K. Lassila-Perini, S. Lehti, T. Lindén, P. Luukka, T. Peltola, E. Tuominen, J. Tuominiemi, E. Tuovinen, L. Wendland

Helsinki Institute of Physics, Helsinki, Finland

J. Talvitie, T. Tuuva

Lappeenranta University of Technology, Lappeenranta, Finland

M. Besancon, F. Couderc, M. Dejardin, D. Denegri, B. Fabbro, J.L. Faure, C. Favaro, F. Ferri, S. Ganjour, A. Givernaud, P. Gras, G. Hamel de Monchenault, P. Jarry, E. Locci, M. Machet, J. Malcles, J. Rander, A. Rosowsky, M. Titov, A. Zghiche

IRFU, CEA, Université Paris-Saclay, Gif-sur-Yvette, France

I. Antropov, S. Baffioni, F. Beaudette, P. Busson, L. Cadamuro, E. Chapon, C. Charlot, O. Davignon, N. Filipovic, R. Granier de Cassagnac, M. Jo, S. Lisniak, L. Mastrolorenzo, P. Miné, I.N. Naranjo, M. Nguyen, C. Ochando, G. Ortona, P. Paganini, P. Pigard, S. Regnard, R. Salerno, J.B. Sauvan, Y. Sirois, T. Strebler, Y. Yilmaz, A. Zabi

Laboratoire Leprince-Ringuet, Ecole Polytechnique, IN2P3-CNRS, Palaiseau, France

J.-L. Agram [15], J. Andrea, A. Aubin, D. Bloch, J.-M. Brom, M. Buttignol, E.C. Chabert, N. Chanon, C. Collard, E. Conte [15], X. Coubez, J.-C. Fontaine [15], D. Gelé, U. Goerlach, C. Goetzmann, A.-C. Le Bihan, J.A. Merlin [2], K. Skovpen, P. Van Hove

Institut Pluridisciplinaire Hubert Curien, Université de Strasbourg, Université de Haute Alsace Mulhouse, CNRS/IN2P3, Strasbourg, France

S. Gadrat

Centre de Calcul de l'Institut National de Physique Nucleaire et de Physique des Particules, CNRS/IN2P3, Villeurbanne, France

S. Beauceron, C. Bernet, G. Boudoul, E. Bouvier, C.A. Carrillo Montoya, R. Chierici, D. Contardo, B. Courbon, P. Depasse, H. El Mamouni, J. Fan, J. Fay, S. Gascon, M. Gouzevitch, B. Ille, F. Lagarde, I.B. Laktineh, M. Lethuillier, L. Mirabito, A.L. Pequegnot, S. Perries, J.D. Ruiz Alvarez, D. Sabes, L. Sgandurra, V. Sordini, M. Vander Donckt, P. Verdier, S. Viret

Université de Lyon, Université Claude Bernard Lyon 1, CNRS-IN2P3, Institut de Physique Nucléaire de Lyon, Villeurbanne, France

T. Toriashvili [16]

Georgian Technical University, Tbilisi, Georgia

Z. Tsamalaidze [10]

Tbilisi State University, Tbilisi, Georgia

C. Autermann, S. Beranek, L. Feld, A. Heister, M.K. Kiesel, K. Klein, M. Lipinski, A. Ostapchuk, M. Preuten, F. Raupach, S. Schael, J.F. Schulte, T. Verlage, H. Weber, V. Zhukov [6]

RWTH Aachen University, I. Physikalisches Institut, Aachen, Germany

M. Ata, M. Brodski, E. Dietz-Laursonn, D. Duchardt, M. Endres, M. Erdmann, S. Erdweg, T. Esch, R. Fischer, A. Güth, T. Hebbeker, C. Heidemann, K. Hoepfner, S. Knutzen, P. Kreuzer, M. Merschmeyer, A. Meyer, P. Millet, M. Olschewski, K. Padeken, P. Papacz, T. Pook, M. Radziej, H. Reithler, M. Rieger, F. Scheuch, L. Sonnenschein, D. Teyssier, S. Thüer

RWTH Aachen University, III. Physikalisches Institut A, Aachen, Germany

V. Cherepanov, Y. Erdogan, G. Flügge, H. Geenen, M. Geisler, F. Hoehle, B. Kargoll, T. Kress, Y. Kuessel, A. Künsken, J. Lingemann, A. Nehrkorn, A. Nowack, I.M. Nugent, C. Pistone, O. Pooth, A. Stahl

RWTH Aachen University, III. Physikalisches Institut B, Aachen, Germany

M. Aldaya Martin, I. Asin, N. Bartosik, O. Behnke, U. Behrens, A.J. Bell, K. Borras [17], A. Burgmeier, A. Campbell, F. Costanza, C. Diez Pardos, G. Dolinska, S. Dooling, T. Dorland, G. Eckerlin, D. Eckstein, T. Eichhorn, G. Flucke, E. Gallo [18], J. Garay Garcia, A. Geiser, A. Gizhko, P. Gunnellini, J. Hauk, M. Hempel [19], H. Jung, A. Kalogeropoulos, O. Karacheban [19], M. Kasemann, P. Katsas, J. Kieseler, C. Kleinwort, I. Korol, W. Lange, J. Leonard, K. Lipka, A. Lobanov, W. Lohmann [19], R. Mankel, I. Marfin [19], I.-A. Melzer-Pellmann, A.B. Meyer, G. Mittag, J. Mnich, A. Mussgiller, S. Naumann-Emme, A. Nayak, E. Ntomari, H. Perrey, D. Pitzl, R. Placakyte, A. Raspereza, B. Roland, M.Ö. Sahin, P. Saxena, T. Schoerner-Sadenius, M. Schröder, C. Seitz, S. Spannagel, K.D. Trippkewitz, R. Walsh, C. Wissing

Deutsches Elektronen-Synchrotron, Hamburg, Germany

V. Blobel, M. Centis Vignali, A.R. Draeger, J. Erfle, E. Garutti, K. Goebel, D. Gonzalez, M. Görner, J. Haller, M. Hoffmann, R.S. Höing, A. Junkes, R. Klanner, R. Kogler, N. Kovalchuk, T. Lapsien, T. Lenz, I. Marchesini, D. Marconi, M. Meyer, D. Nowatschin, J. Ott, F. Pantaleo [2], T. Peiffer, A. Perieanu, N. Pietsch, J. Poehlsen, D. Rathjens, C. Sander, C. Scharf, H. Schettler, P. Schleper, E. Schlieckau, A. Schmidt, J. Schwandt, V. Sola, H. Stadie, G. Steinbrück, H. Tholen, D. Troendle, E. Usai, L. Vanelderen, A. Vanhoefer, B. Vormwald

University of Hamburg, Hamburg, Germany

C. Barth, C. Baus, J. Berger, C. Böser, E. Butz, T. Chwalek, F. Colombo, W. De Boer, A. Descroix, A. Dierlamm, S. Fink, F. Frensch, R. Friese, M. Giffels, A. Gilbert, D. Haitz, F. Hartmann [2], S.M. Heindl, U. Husemann, I. Katkov [6], A. Kornmayer [2], P. Lobelle Pardo, B. Maier, H. Mildner, M.U. Mozer, T. Müller, Th. Müller, M. Plagge, G. Quast, K. Rabbertz, S. Röcker, F. Roscher, G. Sieber, H.J. Simonis, F.M. Stober, R. Ulrich, J. Wagner-Kuhr, S. Wayand, M. Weber, T. Weiler, S. Williamson, C. Wöhrmann, R. Wolf

Institut für Experimentelle Kernphysik, Karlsruhe, Germany

G. Anagnostou, G. Daskalakis, T. Geralis, V.A. Giakoumopoulou, A. Kyriakis, D. Loukas, A. Psallidas, I. Topsis-Giotis

Institute of Nuclear and Particle Physics (INPP), NCSR Demokritos, Aghia Paraskevi, Greece

A. Agapitos, S. Kesisoglou, A. Panagiotou, N. Saoulidou, E. Tziaferi

National and Kapodistrian University of Athens, Athens, Greece

I. Evangelou, G. Flouris, C. Foudas, P. Kokkas, N. Loukas, N. Manthos, I. Papadopoulos, E. Paradas, J. Strologas

University of Ioánnina, Ioánnina, Greece

G. Bencze, C. Hajdu, A. Hazi, P. Hidas, D. Horvath [20], F. Sikler, V. Veszpremi, G. Vesztergombi [21], A.J. Zsigmond

Wigner Research Centre for Physics, Budapest, Hungary

N. Beni, S. Czellar, J. Karancsi [22], J. Molnar, Z. Szillasi [2]

Institute of Nuclear Research ATOMKI, Debrecen, Hungary

M. Bartók [23], A. Makovec, P. Raics, Z.L. Trocsanyi, B. Ujvari

University of Debrecen, Debrecen, Hungary

S. Choudhury [24], P. Mal, K. Mandal, D.K. Sahoo, N. Sahoo, S.K. Swain

National Institute of Science Education and Research, Bhubaneswar, India

S. Bansal, S.B. Beri, V. Bhatnagar, R. Chawla, R. Gupta, U. Bhawandeep, A.K. Kalsi, A. Kaur, M. Kaur, R. Kumar, A. Mehta, M. Mittal, J.B. Singh, G. Walia

Panjab University, Chandigarh, India

Ashok Kumar, A. Bhardwaj, B.C. Choudhary, R.B. Garg, A. Kumar, S. Malhotra, M. Naimuddin, N. Nishu, K. Ranjan, R. Sharma, V. Sharma

University of Delhi, Delhi, India

S. Bhattacharya, K. Chatterjee, S. Dey, S. Dutta, Sa. Jain, N. Majumdar, A. Modak, K. Mondal, S. Mukherjee, S. Mukhopadhyay, A. Roy, D. Roy, S. Roy Chowdhury, S. Sarkar, M. Sharan

Saha Institute of Nuclear Physics, Kolkata, India

A. Abdulsalam, R. Chudasama, D. Dutta, V. Jha, V. Kumar, A.K. Mohanty [2], L.M. Pant, P. Shukla, A. Topkar

Bhabha Atomic Research Centre, Mumbai, India

T. Aziz, S. Banerjee, S. Bhowmik [25], R.M. Chatterjee, R.K. Dewanjee, S. Dugad, S. Ganguly, S. Ghosh, M. Guchait, A. Gurtu [26], G. Kole, S. Kumar, B. Mahakud, M. Maity [25], G. Majumder, K. Mazumdar, S. Mitra, G.B. Mohanty, B. Parida, T. Sarkar [25], N. Sur, B. Sutar, N. Wickramage [27]

Tata Institute of Fundamental Research, Mumbai, India

S. Chauhan, S. Dube, A. Kapoor, K. Kothekar, S. Sharma

Indian Institute of Science Education and Research (IISER), Pune, India

H. Bakhshiansohi, H. Behnamian, S.M. Etesami [28], A. Fahim [29], R. Goldouzian, M. Khakzad, M. Mohammadi Najafabadi, M. Naseri, S. Paktinat Mehdiabadi, F. Rezaei Hosseinabadi, B. Safarzadeh [30], M. Zeinali

Institute for Research in Fundamental Sciences (IPM), Tehran, Iran

M. Felcini, M. Grunewald

University College Dublin, Dublin, Ireland

M. Abbrescia [a,b], C. Calabria [a,b], C. Caputo [a,b], A. Colaleo [a], D. Creanza [a,c], L. Cristella [a,b], N. De Filippis [a,c], M. De Palma [a,b], L. Fiore [a], G. Iaselli [a,c], G. Maggi [a,c], M. Maggi [a], G. Miniello [a,b], S. My [a,c], S. Nuzzo [a,b], A. Pompili [a,b], G. Pugliese [a,c], R. Radogna [a,b], A. Ranieri [a], G. Selvaggi [a,b], L. Silvestris [a,2], R. Venditti [a,b], P. Verwilligen [a]

[a] *INFN Sezione di Bari, Bari, Italy*
[b] *Università di Bari, Bari, Italy*
[c] *Politecnico di Bari, Bari, Italy*

G. Abbiendi [a], C. Battilana [2], A.C. Benvenuti [a], D. Bonacorsi [a,b], S. Braibant-Giacomelli [a,b], L. Brigliadori [a,b], R. Campanini [a,b], P. Capiluppi [a,b], A. Castro [a,b], F.R. Cavallo [a], S.S. Chhibra [a,b], G. Codispoti [a,b], M. Cuffiani [a,b], G.M. Dallavalle [a], F. Fabbri [a], A. Fanfani [a,b], D. Fasanella [a,b], P. Giacomelli [a], C. Grandi [a], L. Guiducci [a,b], S. Marcellini [a], G. Masetti [a], A. Montanari [a], F.L. Navarria [a,b], A. Perrotta [a], A.M. Rossi [a,b], T. Rovelli [a,b], G.P. Siroli [a,b], N. Tosi [a,b,2], R. Travaglini [a,b]

[a] *INFN Sezione di Bologna, Bologna, Italy*
[b] *Università di Bologna, Bologna, Italy*

G. Cappello [a], M. Chiorboli [a,b], S. Costa [a,b], A. Di Mattia [a], F. Giordano [a,b], R. Potenza [a,b], A. Tricomi [a,b], C. Tuve [a,b]

[a] *INFN Sezione di Catania, Catania, Italy*
[b] *Università di Catania, Catania, Italy*

G. Barbagli [a], V. Ciulli [a,b], C. Civinini [a], R. D'Alessandro [a,b], E. Focardi [a,b], V. Gori [a,b], P. Lenzi [a,b], M. Meschini [a], S. Paoletti [a], G. Sguazzoni [a], L. Viliani [a,b,2]

[a] *INFN Sezione di Firenze, Firenze, Italy*
[b] *Università di Firenze, Firenze, Italy*

L. Benussi, S. Bianco, F. Fabbri, D. Piccolo, F. Primavera [2]

INFN Laboratori Nazionali di Frascati, Frascati, Italy

V. Calvelli [a,b], F. Ferro [a], M. Lo Vetere [a,b], M.R. Monge [a,b], E. Robutti [a], S. Tosi [a,b]

[a] *INFN Sezione di Genova, Genova, Italy*
[b] *Università di Genova, Genova, Italy*

L. Brianza, M.E. Dinardo [a,b], S. Fiorendi [a,b], S. Gennai [a], R. Gerosa [a,b], A. Ghezzi [a,b], P. Govoni [a,b],
S. Malvezzi [a], R.A. Manzoni [a,b,2], B. Marzocchi [a,b], D. Menasce [a], L. Moroni [a], M. Paganoni [a,b], D. Pedrini [a],
S. Ragazzi [a,b], N. Redaelli [a], T. Tabarelli de Fatis [a,b]

[a] *INFN Sezione di Milano-Bicocca, Milano, Italy*
[b] *Università di Milano-Bicocca, Milano, Italy*

S. Buontempo [a], N. Cavallo [a,c], S. Di Guida [a,d,2], M. Esposito [a,b], F. Fabozzi [a,c], A.O.M. Iorio [a,b], G. Lanza [a],
L. Lista [a], S. Meola [a,d,2], M. Merola [a], P. Paolucci [a,2], C. Sciacca [a,b], F. Thyssen

[a] *INFN Sezione di Napoli, Napoli, Italy*
[b] *Università di Napoli 'Federico II', Napoli, Italy*
[c] *Università della Basilicata, Potenza, Italy*
[d] *Università G. Marconi, Roma, Italy*

P. Azzi [a,2], N. Bacchetta [a], L. Benato [a,b], D. Bisello [a,b], A. Boletti [a,b], A. Branca [a,b], R. Carlin [a,b], P. Checchia [a],
M. Dall'Osso [a,b,2], T. Dorigo [a], U. Dosselli [a], F. Fanzago [a], F. Gasparini [a,b], U. Gasparini [a,b], A. Gozzelino [a],
K. Kanishchev [a,c], S. Lacaprara [a], M. Margoni [a,b], A.T. Meneguzzo [a,b], J. Pazzini [a,b,2], N. Pozzobon [a,b],
P. Ronchese [a,b], F. Simonetto [a,b], E. Torassa [a], M. Tosi [a,b], M. Zanetti, P. Zotto [a,b], A. Zucchetta [a,b,2],
G. Zumerle [a,b]

[a] *INFN Sezione di Padova, Padova, Italy*
[b] *Università di Padova, Padova, Italy*
[c] *Università di Trento, Trento, Italy*

A. Braghieri [a], A. Magnani [a,b], P. Montagna [a,b], S.P. Ratti [a,b], V. Re [a], C. Riccardi [a,b], P. Salvini [a], I. Vai [a,b],
P. Vitulo [a,b]

[a] *INFN Sezione di Pavia, Pavia, Italy*
[b] *Università di Pavia, Pavia, Italy*

L. Alunni Solestizi [a,b], G.M. Bilei [a], D. Ciangottini [a,b,2], L. Fanò [a,b], P. Lariccia [a,b], G. Mantovani [a,b],
M. Menichelli [a], A. Saha [a], A. Santocchia [a,b]

[a] *INFN Sezione di Perugia, Perugia, Italy*
[b] *Università di Perugia, Perugia, Italy*

K. Androsov [a,31], P. Azzurri [a,2], G. Bagliesi [a], J. Bernardini [a], T. Boccali [a], R. Castaldi [a], M.A. Ciocci [a,31],
R. Dell'Orso [a], S. Donato [a,c,2], G. Fedi, L. Foà [a,c,†], A. Giassi [a], M.T. Grippo [a,31], F. Ligabue [a,c], T. Lomtadze [a],
L. Martini [a,b], A. Messineo [a,b], F. Palla [a], A. Rizzi [a,b], A. Savoy-Navarro [a,32], A.T. Serban [a], P. Spagnolo [a],
R. Tenchini [a], G. Tonelli [a,b], A. Venturi [a], P.G. Verdini [a]

[a] *INFN Sezione di Pisa, Pisa, Italy*
[b] *Università di Pisa, Pisa, Italy*
[c] *Scuola Normale Superiore di Pisa, Pisa, Italy*

L. Barone [a,b], F. Cavallari [a], G. D'imperio [a,b,2], D. Del Re [a,b,2], M. Diemoz [a], S. Gelli [a,b], C. Jorda [a],
E. Longo [a,b], F. Margaroli [a,b], P. Meridiani [a], G. Organtini [a,b], R. Paramatti [a], F. Preiato [a,b], S. Rahatlou [a,b],
C. Rovelli [a], F. Santanastasio [a,b], P. Traczyk [a,b,2]

[a] *INFN Sezione di Roma, Roma, Italy*
[b] *Università di Roma, Roma, Italy*

N. Amapane [a,b], R. Arcidiacono [a,c,2], S. Argiro [a,b], M. Arneodo [a,c], R. Bellan [a,b], C. Biino [a], N. Cartiglia [a],
M. Costa [a,b], R. Covarelli [a,b], A. Degano [a,b], N. Demaria [a], L. Finco [a,b,2], B. Kiani [a,b], C. Mariotti [a], S. Maselli [a],

E. Migliore [a,b], V. Monaco [a,b], E. Monteil [a,b], M.M. Obertino [a,b], L. Pacher [a,b], N. Pastrone [a], M. Pelliccioni [a], G.L. Pinna Angioni [a,b], F. Ravera [a,b], A. Romero [a,b], M. Ruspa [a,c], R. Sacchi [a,b], A. Solano [a,b], A. Staiano [a]

[a] *INFN Sezione di Torino, Torino, Italy*
[b] *Università di Torino, Torino, Italy*
[c] *Università del Piemonte Orientale, Novara, Italy*

S. Belforte [a], V. Candelise [a,b], M. Casarsa [a], F. Cossutti [a], G. Della Ricca [a,b], B. Gobbo [a], C. La Licata [a,b], M. Marone [a,b], A. Schizzi [a,b], A. Zanetti [a]

[a] *INFN Sezione di Trieste, Trieste, Italy*
[b] *Università di Trieste, Trieste, Italy*

A. Kropivnitskaya, S.K. Nam

Kangwon National University, Chunchon, Republic of Korea

D.H. Kim, G.N. Kim, M.S. Kim, D.J. Kong, S. Lee, Y.D. Oh, A. Sakharov, D.C. Son

Kyungpook National University, Daegu, Republic of Korea

J.A. Brochero Cifuentes, H. Kim, T.J. Kim [33]

Chonbuk National University, Jeonju, Republic of Korea

S. Song

Chonnam National University, Institute for Universe and Elementary Particles, Kwangju, Republic of Korea

S. Choi, Y. Go, D. Gyun, B. Hong, H. Kim, Y. Kim, B. Lee, K. Lee, K.S. Lee, S. Lee, S.K. Park, Y. Roh

Korea University, Seoul, Republic of Korea

H.D. Yoo

Seoul National University, Seoul, Republic of Korea

M. Choi, H. Kim, J.H. Kim, J.S.H. Lee, I.C. Park, G. Ryu, M.S. Ryu

University of Seoul, Seoul, Republic of Korea

Y. Choi, J. Goh, D. Kim, E. Kwon, J. Lee, I. Yu

Sungkyunkwan University, Suwon, Republic of Korea

V. Dudenas, A. Juodagalvis, J. Vaitkus

Vilnius University, Vilnius, Lithuania

I. Ahmed, Z.A. Ibrahim, J.R. Komaragiri, M.A.B. Md Ali [34], F. Mohamad Idris [35], W.A.T. Wan Abdullah, M.N. Yusli

National Centre for Particle Physics, Universiti Malaya, Kuala Lumpur, Malaysia

E. Casimiro Linares, H. Castilla-Valdez, E. De La Cruz-Burelo, I. Heredia-De La Cruz [36], A. Hernandez-Almada, R. Lopez-Fernandez, A. Sanchez-Hernandez

Centro de Investigacion y de Estudios Avanzados del IPN, Mexico City, Mexico

S. Carrillo Moreno, F. Vazquez Valencia

Universidad Iberoamericana, Mexico City, Mexico

I. Pedraza, H.A. Salazar Ibarguen

Benemerita Universidad Autonoma de Puebla, Puebla, Mexico

A. Morelos Pineda

Universidad Autónoma de San Luis Potosí, San Luis Potosí, Mexico

D. Krofcheck

University of Auckland, Auckland, New Zealand

P.H. Butler

University of Canterbury, Christchurch, New Zealand

A. Ahmad, M. Ahmad, Q. Hassan, H.R. Hoorani, W.A. Khan, T. Khurshid, M. Shoaib

National Centre for Physics, Quaid-I-Azam University, Islamabad, Pakistan

H. Bialkowska, M. Bluj, B. Boimska, T. Frueboes, M. Górski, M. Kazana, K. Nawrocki, K. Romanowska-Rybinska, M. Szleper, P. Zalewski

National Centre for Nuclear Research, Swierk, Poland

G. Brona, K. Bunkowski, A. Byszuk [37], K. Doroba, A. Kalinowski, M. Konecki, J. Krolikowski, M. Misiura, M. Olszewski, M. Walczak

Institute of Experimental Physics, Faculty of Physics, University of Warsaw, Warsaw, Poland

P. Bargassa, C. Beirão Da Cruz E Silva, A. Di Francesco, P. Faccioli, P.G. Ferreira Parracho, M. Gallinaro, N. Leonardo, L. Lloret Iglesias, F. Nguyen, J. Rodrigues Antunes, J. Seixas, O. Toldaiev, D. Vadruccio, J. Varela, P. Vischia

Laboratório de Instrumentação e Física Experimental de Partículas, Lisboa, Portugal

P. Bunin, I. Golutvin, N. Gorbounov, I. Gorbunov, V. Karjavin, V. Konoplyanikov, G. Kozlov, A. Lanev, A. Malakhov, V. Matveev [38,39], P. Moisenz, V. Palichik, V. Perelygin, M. Savina, S. Shmatov, S. Shulha, N. Skatchkov, V. Smirnov, A. Zarubin

Joint Institute for Nuclear Research, Dubna, Russia

V. Golovtsov, Y. Ivanov, V. Kim [40], E. Kuznetsova, P. Levchenko, V. Murzin, V. Oreshkin, I. Smirnov, V. Sulimov, L. Uvarov, S. Vavilov, A. Vorobyev

Petersburg Nuclear Physics Institute, Gatchina (St. Petersburg), Russia

Yu. Andreev, A. Dermenev, S. Gninenko, N. Golubev, A. Karneyeu, M. Kirsanov, N. Krasnikov, A. Pashenkov, D. Tlisov, A. Toropin

Institute for Nuclear Research, Moscow, Russia

V. Epshteyn, V. Gavrilov, N. Lychkovskaya, V. Popov, I. Pozdnyakov, G. Safronov, A. Spiridonov, E. Vlasov, A. Zhokin

Institute for Theoretical and Experimental Physics, Moscow, Russia

A. Bylinkin

National Research Nuclear University 'Moscow Engineering Physics Institute' (MEPhI), Moscow, Russia

V. Andreev, M. Azarkin [39], I. Dremin [39], M. Kirakosyan, A. Leonidov [39], G. Mesyats, S.V. Rusakov

P.N. Lebedev Physical Institute, Moscow, Russia

A. Baskakov, A. Belyaev, E. Boos, M. Dubinin [41], L. Dudko, A. Ershov, A. Gribushin, V. Klyukhin, O. Kodolova, I. Lokhtin, I. Myagkov, S. Obraztsov, S. Petrushanko, V. Savrin, A. Snigirev

Skobeltsyn Institute of Nuclear Physics, Lomonosov Moscow State University, Moscow, Russia

I. Azhgirey, I. Bayshev, S. Bitioukov, V. Kachanov, A. Kalinin, D. Konstantinov, V. Krychkine, V. Petrov, R. Ryutin, A. Sobol, L. Tourtchanovitch, S. Troshin, N. Tyurin, A. Uzunian, A. Volkov

State Research Center of Russian Federation, Institute for High Energy Physics, Protvino, Russia

P. Adzic [42], P. Cirkovic, J. Milosevic, V. Rekovic

University of Belgrade, Faculty of Physics and Vinca Institute of Nuclear Sciences, Belgrade, Serbia

J. Alcaraz Maestre, E. Calvo, M. Cerrada, M. Chamizo Llatas, N. Colino, B. De La Cruz, A. Delgado Peris, A. Escalante Del Valle, C. Fernandez Bedoya, J.P. Fernández Ramos, J. Flix, M.C. Fouz, P. Garcia-Abia, O. Gonzalez Lopez, S. Goy Lopez, J.M. Hernandez, M.I. Josa, E. Navarro De Martino, A. Pérez-Calero Yzquierdo, J. Puerta Pelayo, A. Quintario Olmeda, I. Redondo, L. Romero, J. Santaolalla, M.S. Soares

Centro de Investigaciones Energéticas Medioambientales y Tecnológicas (CIEMAT), Madrid, Spain

C. Albajar, J.F. de Trocóniz, M. Missiroli, D. Moran

Universidad Autónoma de Madrid, Madrid, Spain

J. Cuevas, J. Fernandez Menendez, S. Folgueras, I. Gonzalez Caballero, E. Palencia Cortezon, J.M. Vizan Garcia

Universidad de Oviedo, Oviedo, Spain

I.J. Cabrillo, A. Calderon, J.R. Castiñeiras De Saa, P. De Castro Manzano, M. Fernandez, J. Garcia-Ferrero, G. Gomez, A. Lopez Virto, J. Marco, R. Marco, C. Martinez Rivero, F. Matorras, J. Piedra Gomez, T. Rodrigo, A.Y. Rodríguez-Marrero, A. Ruiz-Jimeno, L. Scodellaro, N. Trevisani, I. Vila, R. Vilar Cortabitarte

Instituto de Física de Cantabria (IFCA), CSIC-Universidad de Cantabria, Santander, Spain

D. Abbaneo, E. Auffray, G. Auzinger, M. Bachtis, P. Baillon, A.H. Ball, D. Barney, A. Benaglia, J. Bendavid, L. Benhabib, J.F. Benitez, G.M. Berruti, P. Bloch, A. Bocci, A. Bonato, C. Botta, H. Breuker, T. Camporesi, R. Castello, G. Cerminara, M. D'Alfonso, D. d'Enterria, A. Dabrowski, V. Daponte, A. David, M. De Gruttola, F. De Guio, A. De Roeck, S. De Visscher, E. Di Marco [43], M. Dobson, M. Dordevic, B. Dorney, T. du Pree, D. Duggan, M. Dünser, N. Dupont, A. Elliott-Peisert, G. Franzoni, J. Fulcher, W. Funk, D. Gigi, K. Gill, D. Giordano, M. Girone, F. Glege, R. Guida, S. Gundacker, M. Guthoff, J. Hammer, P. Harris, J. Hegeman, V. Innocente, P. Janot, H. Kirschenmann, M.J. Kortelainen, K. Kousouris, K. Krajczar, P. Lecoq, C. Lourenço, M.T. Lucchini, N. Magini, L. Malgeri, M. Mannelli, A. Martelli, L. Masetti, F. Meijers, S. Mersi, E. Meschi, F. Moortgat, S. Morovic, M. Mulders, M.V. Nemallapudi, H. Neugebauer, S. Orfanelli [44], L. Orsini, L. Pape, E. Perez, M. Peruzzi, A. Petrilli, G. Petrucciani, A. Pfeiffer, M. Pierini, D. Piparo, A. Racz, T. Reis, G. Rolandi [45], M. Rovere, M. Ruan, H. Sakulin, C. Schäfer, C. Schwick, M. Seidel, A. Sharma, P. Silva, M. Simon, P. Sphicas [46], J. Steggemann, B. Stieger, M. Stoye, Y. Takahashi, D. Treille, A. Triossi, A. Tsirou, G.I. Veres [21], N. Wardle, H.K. Wöhri, A. Zagozdzinska [37], W.D. Zeuner

CERN, European Organization for Nuclear Research, Geneva, Switzerland

W. Bertl, K. Deiters, W. Erdmann, R. Horisberger, Q. Ingram, H.C. Kaestli, D. Kotlinski, U. Langenegger, D. Renker, T. Rohe

Paul Scherrer Institut, Villigen, Switzerland

F. Bachmair, L. Bäni, L. Bianchini, B. Casal, G. Dissertori, M. Dittmar, M. Donegà, P. Eller, C. Grab, C. Heidegger, D. Hits, J. Hoss, G. Kasieczka, W. Lustermann, B. Mangano, M. Marionneau, P. Martinez Ruiz del Arbol, M. Masciovecchio, D. Meister, F. Micheli, P. Musella, F. Nessi-Tedaldi, F. Pandolfi, J. Pata, F. Pauss, L. Perrozzi, M. Quittnat, M. Rossini, M. Schönenberger, A. Starodumov [47], M. Takahashi, V.R. Tavolaro, K. Theofilatos, R. Wallny

Institute for Particle Physics, ETH Zurich, Zurich, Switzerland

T.K. Aarrestad, C. Amsler [48], L. Caminada, M.F. Canelli, V. Chiochia, A. De Cosa, C. Galloni, A. Hinzmann, T. Hreus, B. Kilminster, C. Lange, J. Ngadiuba, D. Pinna, G. Rauco, P. Robmann, F.J. Ronga, D. Salerno, Y. Yang

Universität Zürich, Zurich, Switzerland

M. Cardaci, K.H. Chen, T.H. Doan, Sh. Jain, R. Khurana, M. Konyushikhin, C.M. Kuo, W. Lin, Y.J. Lu, A. Pozdnyakov, S.S. Yu

National Central University, Chung-Li, Taiwan

Arun Kumar, R. Bartek, P. Chang, Y.H. Chang, Y.W. Chang, Y. Chao, K.F. Chen, P.H. Chen, C. Dietz, F. Fiori, U. Grundler, W.-S. Hou, Y. Hsiung, Y.F. Liu, R.-S. Lu, M. Miñano Moya, E. Petrakou, J.f. Tsai, Y.M. Tzeng

National Taiwan University (NTU), Taipei, Taiwan

B. Asavapibhop, K. Kovitanggoon, G. Singh, N. Srimanobhas, N. Suwonjandee

Chulalongkorn University, Faculty of Science, Department of Physics, Bangkok, Thailand

A. Adiguzel, M.N. Bakirci [49], Z.S. Demiroglu, C. Dozen, F.H. Gecit, S. Girgis, G. Gokbulut, Y. Guler, E. Gurpinar, I. Hos, E.E. Kangal [50], A. Kayis Topaksu, G. Onengut [51], M. Ozcan, K. Ozdemir [52], S. Ozturk [49], D. Sunar Cerci [53], B. Tali [53], H. Topakli [49], M. Vergili, C. Zorbilmez

Cukurova University, Adana, Turkey

I.V. Akin, B. Bilin, S. Bilmis, B. Isildak [54], G. Karapinar [55], M. Yalvac, M. Zeyrek

Middle East Technical University, Physics Department, Ankara, Turkey

E. Gülmez, M. Kaya [56], O. Kaya [57], E.A. Yetkin [58], T. Yetkin [59]

Bogazici University, Istanbul, Turkey

A. Cakir, K. Cankocak, S. Sen [60], F.I. Vardarlı

Istanbul Technical University, Istanbul, Turkey

B. Grynyov

Institute for Scintillation Materials of National Academy of Science of Ukraine, Kharkov, Ukraine

L. Levchuk, P. Sorokin

National Scientific Center, Kharkov Institute of Physics and Technology, Kharkov, Ukraine

R. Aggleton, F. Ball, L. Beck, J.J. Brooke, E. Clement, D. Cussans, H. Flacher, J. Goldstein, M. Grimes, G.P. Heath, H.F. Heath, J. Jacob, L. Kreczko, C. Lucas, Z. Meng, D.M. Newbold [61], S. Paramesvaran, A. Poll, T. Sakuma, S. Seif El Nasr-storey, S. Senkin, D. Smith, V.J. Smith

University of Bristol, Bristol, United Kingdom

K.W. Bell, A. Belyaev [62], C. Brew, R.M. Brown, L. Calligaris, D. Cieri, D.J.A. Cockerill, J.A. Coughlan, K. Harder, S. Harper, E. Olaiya, D. Petyt, C.H. Shepherd-Themistocleous, A. Thea, I.R. Tomalin, T. Williams, S.D. Worm

Rutherford Appleton Laboratory, Didcot, United Kingdom

M. Baber, R. Bainbridge, O. Buchmuller, A. Bundock, D. Burton, S. Casasso, M. Citron, D. Colling, L. Corpe, P. Dauncey, G. Davies, A. De Wit, M. Della Negra, P. Dunne, A. Elwood, D. Futyan, G. Hall, G. Iles, R. Lane, R. Lucas [61], L. Lyons, A.-M. Magnan, S. Malik, J. Nash, A. Nikitenko [47], J. Pela, M. Pesaresi, K. Petridis, D.M. Raymond, A. Richards, A. Rose, C. Seez, A. Tapper, K. Uchida, M. Vazquez Acosta [63], T. Virdee, S.C. Zenz

Imperial College, London, United Kingdom

J.E. Cole, P.R. Hobson, A. Khan, P. Kyberd, D. Leggat, D. Leslie, I.D. Reid, P. Symonds, L. Teodorescu, M. Turner

Brunel University, Uxbridge, United Kingdom

A. Borzou, K. Call, J. Dittmann, K. Hatakeyama, H. Liu, N. Pastika

Baylor University, Waco, USA

O. Charaf, S.I. Cooper, C. Henderson, P. Rumerio

The University of Alabama, Tuscaloosa, USA

D. Arcaro, A. Avetisyan, T. Bose, C. Fantasia, D. Gastler, P. Lawson, D. Rankin, C. Richardson, J. Rohlf, J. St. John, L. Sulak, D. Zou

Boston University, Boston, USA

J. Alimena, E. Berry, S. Bhattacharya, D. Cutts, A. Ferapontov, A. Garabedian, J. Hakala, U. Heintz, E. Laird, G. Landsberg, Z. Mao, M. Narain, S. Piperov, S. Sagir, R. Syarif

Brown University, Providence, USA

R. Breedon, G. Breto, M. Calderon De La Barca Sanchez, S. Chauhan, M. Chertok, J. Conway, R. Conway, P.T. Cox, R. Erbacher, G. Funk, M. Gardner, W. Ko, R. Lander, C. Mclean, M. Mulhearn, D. Pellett, J. Pilot, F. Ricci-Tam, S. Shalhout, J. Smith, M. Squires, D. Stolp, M. Tripathi, S. Wilbur, R. Yohay

University of California, Davis, Davis, USA

R. Cousins, P. Everaerts, A. Florent, J. Hauser, M. Ignatenko, D. Saltzberg, E. Takasugi, V. Valuev, M. Weber

University of California, Los Angeles, USA

K. Burt, R. Clare, J. Ellison, J.W. Gary, G. Hanson, J. Heilman, M. Ivova Paneva, P. Jandir, E. Kennedy, F. Lacroix, O.R. Long, A. Luthra, M. Malberti, M. Olmedo Negrete, A. Shrinivas, H. Wei, S. Wimpenny, B.R. Yates

University of California, Riverside, Riverside, USA

J.G. Branson, G.B. Cerati, S. Cittolin, R.T. D'Agnolo, M. Derdzinski, A. Holzner, R. Kelley, D. Klein, J. Letts, I. Macneill, D. Olivito, S. Padhi, M. Pieri, M. Sani, V. Sharma, S. Simon, M. Tadel, A. Vartak, S. Wasserbaech [64], C. Welke, F. Würthwein, A. Yagil, G. Zevi Della Porta

University of California, San Diego, La Jolla, USA

J. Bradmiller-Feld, C. Campagnari, A. Dishaw, V. Dutta, K. Flowers, M. Franco Sevilla, P. Geffert, C. George, F. Golf, L. Gouskos, J. Gran, J. Incandela, N. Mccoll, S.D. Mullin, J. Richman, D. Stuart, I. Suarez, C. West, J. Yoo

University of California, Santa Barbara, Santa Barbara, USA

D. Anderson, A. Apresyan, A. Bornheim, J. Bunn, Y. Chen, J. Duarte, A. Mott, H.B. Newman, C. Pena, M. Spiropulu, J.R. Vlimant, S. Xie, R.Y. Zhu

California Institute of Technology, Pasadena, USA

M.B. Andrews, V. Azzolini, A. Calamba, B. Carlson, T. Ferguson, M. Paulini, J. Russ, M. Sun, H. Vogel, I. Vorobiev

Carnegie Mellon University, Pittsburgh, USA

J.P. Cumalat, W.T. Ford, A. Gaz, F. Jensen, A. Johnson, M. Krohn, T. Mulholland, U. Nauenberg, K. Stenson, S.R. Wagner

University of Colorado Boulder, Boulder, USA

J. Alexander, A. Chatterjee, J. Chaves, J. Chu, S. Dittmer, N. Eggert, N. Mirman, G. Nicolas Kaufman, J.R. Patterson, A. Rinkevicius, A. Ryd, L. Skinnari, L. Soffi, W. Sun, S.M. Tan, W.D. Teo, J. Thom, J. Thompson, J. Tucker, Y. Weng, P. Wittich

Cornell University, Ithaca, USA

S. Abdullin, M. Albrow, G. Apollinari, S. Banerjee, L.A.T. Bauerdick, A. Beretvas, J. Berryhill, P.C. Bhat, G. Bolla, K. Burkett, J.N. Butler, H.W.K. Cheung, F. Chlebana, S. Cihangir, V.D. Elvira, I. Fisk, J. Freeman, E. Gottschalk, L. Gray, D. Green, S. Grünendahl, O. Gutsche, J. Hanlon, D. Hare, R.M. Harris, S. Hasegawa, J. Hirschauer, Z. Hu, B. Jayatilaka, S. Jindariani, M. Johnson, U. Joshi, B. Klima, B. Kreis, S. Lammel, J. Linacre, D. Lincoln, R. Lipton, T. Liu, R. Lopes De Sá, J. Lykken, K. Maeshima, J.M. Marraffino, S. Maruyama, D. Mason, P. McBride, P. Merkel, K. Mishra, S. Mrenna, S. Nahn, C. Newman-Holmes [†], V. O'Dell, K. Pedro, O. Prokofyev, G. Rakness, E. Sexton-Kennedy, A. Soha, W.J. Spalding, L. Spiegel, N. Strobbe, L. Taylor, S. Tkaczyk, N.V. Tran, L. Uplegger, E.W. Vaandering, C. Vernieri, M. Verzocchi, R. Vidal, H.A. Weber, A. Whitbeck

Fermi National Accelerator Laboratory, Batavia, USA

D. Acosta, P. Avery, P. Bortignon, D. Bourilkov, A. Carnes, M. Carver, D. Curry, S. Das, R.D. Field, I.K. Furic, S.V. Gleyzer, J. Konigsberg, A. Korytov, K. Kotov, P. Ma, K. Matchev, H. Mei, P. Milenovic [65], G. Mitselmakher, D. Rank, R. Rossin, L. Shchutska, M. Snowball, D. Sperka, N. Terentyev, L. Thomas, J. Wang, S. Wang, J. Yelton

University of Florida, Gainesville, USA

S. Hewamanage, S. Linn, P. Markowitz, G. Martinez, J.L. Rodriguez

Florida International University, Miami, USA

A. Ackert, J.R. Adams, T. Adams, A. Askew, S. Bein, J. Bochenek, B. Diamond, J. Haas, S. Hagopian, V. Hagopian, K.F. Johnson, A. Khatiwada, H. Prosper, M. Weinberg

Florida State University, Tallahassee, USA

M.M. Baarmand, V. Bhopatkar, S. Colafranceschi [66], M. Hohlmann, H. Kalakhety, D. Noonan, T. Roy, F. Yumiceva

Florida Institute of Technology, Melbourne, USA

M.R. Adams, L. Apanasevich, D. Berry, R.R. Betts, I. Bucinskaite, R. Cavanaugh, O. Evdokimov, L. Gauthier, C.E. Gerber, D.J. Hofman, P. Kurt, C. O'Brien, I.D. Sandoval Gonzalez, P. Turner, N. Varelas, Z. Wu, M. Zakaria

University of Illinois at Chicago (UIC), Chicago, USA

B. Bilki [67], W. Clarida, K. Dilsiz, S. Durgut, R.P. Gandrajula, M. Haytmyradov, V. Khristenko, J.-P. Merlo, H. Mermerkaya [68], A. Mestvirishvili, A. Moeller, J. Nachtman, H. Ogul, Y. Onel, F. Ozok [58], A. Penzo, C. Snyder, E. Tiras, J. Wetzel, K. Yi

The University of Iowa, Iowa City, USA

I. Anderson, B.A. Barnett, B. Blumenfeld, N. Eminizer, D. Fehling, L. Feng, A.V. Gritsan, P. Maksimovic, C. Martin, M. Osherson, J. Roskes, A. Sady, U. Sarica, M. Swartz, M. Xiao, Y. Xin, C. You

Johns Hopkins University, Baltimore, USA

P. Baringer, A. Bean, G. Benelli, C. Bruner, R.P. Kenny III, D. Majumder, M. Malek, M. Murray, S. Sanders, R. Stringer, Q. Wang

The University of Kansas, Lawrence, USA

A. Ivanov, K. Kaadze, S. Khalil, M. Makouski, Y. Maravin, A. Mohammadi, L.K. Saini, N. Skhirtladze, S. Toda

Kansas State University, Manhattan, USA

D. Lange, F. Rebassoo, D. Wright

Lawrence Livermore National Laboratory, Livermore, USA

C. Anelli, A. Baden, O. Baron, A. Belloni, B. Calvert, S.C. Eno, C. Ferraioli, J.A. Gomez, N.J. Hadley, S. Jabeen, R.G. Kellogg, T. Kolberg, J. Kunkle, Y. Lu, A.C. Mignerey, Y.H. Shin, A. Skuja, M.B. Tonjes, S.C. Tonwar

University of Maryland, College Park, USA

A. Apyan, R. Barbieri, A. Baty, K. Bierwagen, S. Brandt, W. Busza, I.A. Cali, Z. Demiragli, L. Di Matteo, G. Gomez Ceballos, M. Goncharov, D. Gulhan, Y. Iiyama, G.M. Innocenti, M. Klute, D. Kovalskyi, Y.S. Lai, Y.-J. Lee, A. Levin, P.D. Luckey, A.C. Marini, C. Mcginn, C. Mironov, S. Narayanan, X. Niu, C. Paus, C. Roland, G. Roland, J. Salfeld-Nebgen, G.S.F. Stephans, K. Sumorok, M. Varma, D. Velicanu, J. Veverka, J. Wang, T.W. Wang, B. Wyslouch, M. Yang, V. Zhukova

Massachusetts Institute of Technology, Cambridge, USA

B. Dahmes, A. Evans, A. Finkel, A. Gude, P. Hansen, S. Kalafut, S.C. Kao, K. Klapoetke, Y. Kubota, Z. Lesko, J. Mans, S. Nourbakhsh, N. Ruckstuhl, R. Rusack, N. Tambe, J. Turkewitz

University of Minnesota, Minneapolis, USA

J.G. Acosta, S. Oliveros

University of Mississippi, Oxford, USA

E. Avdeeva, K. Bloom, S. Bose, D.R. Claes, A. Dominguez, C. Fangmeier, R. Gonzalez Suarez, R. Kamalieddin, D. Knowlton, I. Kravchenko, F. Meier, J. Monroy, F. Ratnikov, J.E. Siado, G.R. Snow

University of Nebraska-Lincoln, Lincoln, USA

M. Alyari, J. Dolen, J. George, A. Godshalk, C. Harrington, I. Iashvili, J. Kaisen, A. Kharchilava, A. Kumar, S. Rappoccio, B. Roozbahani

State University of New York at Buffalo, Buffalo, USA

G. Alverson, E. Barberis, D. Baumgartel, M. Chasco, A. Hortiangtham, A. Massironi, D.M. Morse, D. Nash, T. Orimoto, R. Teixeira De Lima, D. Trocino, R.-J. Wang, D. Wood, J. Zhang

Northeastern University, Boston, USA

K.A. Hahn, A. Kubik, J.F. Low, N. Mucia, N. Odell, B. Pollack, M. Schmitt, S. Stoynev, K. Sung, M. Trovato, M. Velasco

Northwestern University, Evanston, USA

A. Brinkerhoff, N. Dev, M. Hildreth, C. Jessop, D.J. Karmgard, N. Kellams, K. Lannon, N. Marinelli, F. Meng, C. Mueller, Y. Musienko [38], M. Planer, A. Reinsvold, R. Ruchti, G. Smith, S. Taroni, N. Valls, M. Wayne, M. Wolf, A. Woodard

University of Notre Dame, Notre Dame, USA

L. Antonelli, J. Brinson, B. Bylsma, L.S. Durkin, S. Flowers, A. Hart, C. Hill, R. Hughes, W. Ji, T.Y. Ling, B. Liu, W. Luo, D. Puigh, M. Rodenburg, B.L. Winer, H.W. Wulsin

The Ohio State University, Columbus, USA

O. Driga, P. Elmer, J. Hardenbrook, P. Hebda, S.A. Koay, P. Lujan, D. Marlow, T. Medvedeva, M. Mooney, J. Olsen, C. Palmer, P. Piroué, H. Saka, D. Stickland, C. Tully, A. Zuranski

Princeton University, Princeton, USA

S. Malik

University of Puerto Rico, Mayaguez, USA

A. Barker, V.E. Barnes, D. Benedetti, D. Bortoletto, L. Gutay, M.K. Jha, M. Jones, A.W. Jung, K. Jung, D.H. Miller, N. Neumeister, B.C. Radburn-Smith, X. Shi, I. Shipsey, D. Silvers, J. Sun, A. Svyatkovskiy, F. Wang, W. Xie, L. Xu

Purdue University, West Lafayette, USA

N. Parashar, J. Stupak

Purdue University Calumet, Hammond, USA

A. Adair, B. Akgun, Z. Chen, K.M. Ecklund, F.J.M. Geurts, M. Guilbaud, W. Li, B. Michlin, M. Northup, B.P. Padley, R. Redjimi, J. Roberts, J. Rorie, Z. Tu, J. Zabel

Rice University, Houston, USA

B. Betchart, A. Bodek, P. de Barbaro, R. Demina, Y. Eshaq, T. Ferbel, M. Galanti, A. Garcia-Bellido, J. Han, A. Harel, O. Hindrichs, A. Khukhunaishvili, G. Petrillo, P. Tan, M. Verzetti

University of Rochester, Rochester, USA

S. Arora, J.P. Chou, C. Contreras-Campana, E. Contreras-Campana, D. Ferencek, Y. Gershtein, R. Gray, E. Halkiadakis, D. Hidas, E. Hughes, S. Kaplan, R. Kunnawalkam Elayavalli, A. Lath, K. Nash, S. Panwalkar, M. Park, S. Salur, S. Schnetzer, D. Sheffield, S. Somalwar, R. Stone, S. Thomas, P. Thomassen, M. Walker

Rutgers, The State University of New Jersey, Piscataway, USA

M. Foerster, G. Riley, K. Rose, S. Spanier

University of Tennessee, Knoxville, USA

O. Bouhali [69], A. Castaneda Hernandez [69], A. Celik, M. Dalchenko, M. De Mattia, A. Delgado, S. Dildick, R. Eusebi, J. Gilmore, T. Huang, T. Kamon [70], V. Krutelyov, R. Mueller, I. Osipenkov, Y. Pakhotin, R. Patel, A. Perloff, A. Rose, A. Safonov, A. Tatarinov, K.A. Ulmer [2]

Texas A&M University, College Station, USA

N. Akchurin, C. Cowden, J. Damgov, C. Dragoiu, P.R. Dudero, J. Faulkner, S. Kunori, K. Lamichhane, S.W. Lee, T. Libeiro, S. Undleeb, I. Volobouev

Texas Tech University, Lubbock, USA

E. Appelt, A.G. Delannoy, S. Greene, A. Gurrola, R. Janjam, W. Johns, C. Maguire, Y. Mao, A. Melo, H. Ni, P. Sheldon, B. Snook, S. Tuo, J. Velkovska, Q. Xu

Vanderbilt University, Nashville, USA

M.W. Arenton, B. Cox, B. Francis, J. Goodell, R. Hirosky, A. Ledovskoy, H. Li, C. Lin, C. Neu, T. Sinthuprasith, X. Sun, Y. Wang, E. Wolfe, J. Wood, F. Xia

University of Virginia, Charlottesville, USA

C. Clarke, R. Harr, P.E. Karchin, C. Kottachchi Kankanamge Don, P. Lamichhane, J. Sturdy

Wayne State University, Detroit, USA

D.A. Belknap, D. Carlsmith, M. Cepeda, S. Dasu, L. Dodd, S. Duric, B. Gomber, M. Grothe, R. Hall-Wilton, M. Herndon, A. Hervé, P. Klabbers, A. Lanaro, A. Levine, K. Long, R. Loveless, A. Mohapatra, I. Ojalvo, T. Perry, G.A. Pierro, G. Polese, T. Ruggles, T. Sarangi, A. Savin, A. Sharma, N. Smith, W.H. Smith, D. Taylor, N. Woods

University of Wisconsin – Madison, Madison, WI, USA

[†] Deceased.
[1] Also at Vienna University of Technology, Vienna, Austria.
[2] Also at CERN, European Organization for Nuclear Research, Geneva, Switzerland.
[3] Also at State Key Laboratory of Nuclear Physics and Technology, Peking University, Beijing, China.
[4] Also at Institut Pluridisciplinaire Hubert Curien, Université de Strasbourg, Université de Haute Alsace Mulhouse, CNRS/IN2P3, Strasbourg, France.
[5] Also at National Institute of Chemical Physics and Biophysics, Tallinn, Estonia.
[6] Also at Skobeltsyn Institute of Nuclear Physics, Lomonosov Moscow State University, Moscow, Russia.
[7] Also at Universidade Estadual de Campinas, Campinas, Brazil.
[8] Also at Centre National de la Recherche Scientifique (CNRS) – IN2P3, Paris, France.
[9] Also at Laboratoire Leprince-Ringuet, Ecole Polytechnique, IN2P3-CNRS, Palaiseau, France.
[10] Also at Joint Institute for Nuclear Research, Dubna, Russia.
[11] Also at Helwan University, Cairo, Egypt.
[12] Now at Zewail City of Science and Technology, Zewail, Egypt.
[13] Also at British University in Egypt, Cairo, Egypt.
[14] Now at Ain Shams University, Cairo, Egypt.
[15] Also at Université de Haute Alsace, Mulhouse, France.
[16] Also at Tbilisi State University, Tbilisi, Georgia.
[17] Also at RWTH Aachen University, III. Physikalisches Institut A, Aachen, Germany.
[18] Also at University of Hamburg, Hamburg, Germany.
[19] Also at Brandenburg University of Technology, Cottbus, Germany.
[20] Also at Institute of Nuclear Research ATOMKI, Debrecen, Hungary.
[21] Also at Eötvös Loránd University, Budapest, Hungary.
[22] Also at University of Debrecen, Debrecen, Hungary.
[23] Also at Wigner Research Centre for Physics, Budapest, Hungary.
[24] Also at Indian Institute of Science Education and Research, Bhopal, India.
[25] Also at University of Visva-Bharati, Santiniketan, India.
[26] Now at King Abdulaziz University, Jeddah, Saudi Arabia.
[27] Also at University of Ruhuna, Matara, Sri Lanka.
[28] Also at Isfahan University of Technology, Isfahan, Iran.
[29] Also at University of Tehran, Department of Engineering Science, Tehran, Iran.
[30] Also at Plasma Physics Research Center, Science and Research Branch, Islamic Azad University, Tehran, Iran.
[31] Also at Università degli Studi di Siena, Siena, Italy.
[32] Also at Purdue University, West Lafayette, USA.
[33] Now at Hanyang University, Seoul, Korea.
[34] Also at International Islamic University of Malaysia, Kuala Lumpur, Malaysia.
[35] Also at Malaysian Nuclear Agency, MOSTI, Kajang, Malaysia.
[36] Also at Consejo Nacional de Ciencia y Tecnología, Mexico city, Mexico.
[37] Also at Warsaw University of Technology, Institute of Electronic Systems, Warsaw, Poland.
[38] Also at Institute for Nuclear Research, Moscow, Russia.
[39] Now at National Research Nuclear University 'Moscow Engineering Physics Institute' (MEPhI), Moscow, Russia.
[40] Also at St. Petersburg State Polytechnical University, St. Petersburg, Russia.
[41] Also at California Institute of Technology, Pasadena, USA.
[42] Also at Faculty of Physics, University of Belgrade, Belgrade, Serbia.
[43] Also at INFN Sezione di Roma; Università di Roma, Roma, Italy.
[44] Also at National Technical University of Athens, Athens, Greece.
[45] Also at Scuola Normale e Sezione dell'INFN, Pisa, Italy.
[46] Also at National and Kapodistrian University of Athens, Athens, Greece.
[47] Also at Institute for Theoretical and Experimental Physics, Moscow, Russia.
[48] Also at Albert Einstein Center for Fundamental Physics, Bern, Switzerland.
[49] Also at Gaziosmanpasa University, Tokat, Turkey.
[50] Also at Mersin University, Mersin, Turkey.
[51] Also at Cag University, Mersin, Turkey.
[52] Also at Piri Reis University, Istanbul, Turkey.
[53] Also at Adiyaman University, Adiyaman, Turkey.
[54] Also at Ozyegin University, Istanbul, Turkey.
[55] Also at Izmir Institute of Technology, Izmir, Turkey.
[56] Also at Marmara University, Istanbul, Turkey.
[57] Also at Kafkas University, Kars, Turkey.
[58] Also at Mimar Sinan University, Istanbul, Istanbul, Turkey.
[59] Also at Yildiz Technical University, Istanbul, Turkey.
[60] Also at Hacettepe University, Ankara, Turkey.

[61] Also at Rutherford Appleton Laboratory, Didcot, United Kingdom.
[62] Also at School of Physics and Astronomy, University of Southampton, Southampton, United Kingdom.
[63] Also at Instituto de Astrofísica de Canarias, La Laguna, Spain.
[64] Also at Utah Valley University, Orem, USA.
[65] Also at University of Belgrade, Faculty of Physics and Vinca Institute of Nuclear Sciences, Belgrade, Serbia.
[66] Also at Facoltà Ingegneria, Università di Roma, Roma, Italy.
[67] Also at Argonne National Laboratory, Argonne, USA.
[68] Also at Erzincan University, Erzincan, Turkey.
[69] Also at Texas A&M University at Qatar, Doha, Qatar.
[70] Also at Kyungpook National University, Daegu, Korea.